

2017

Roll bonding of metal-polymer-metal sandwich composites

Saeed Mousa
Iowa State University

Follow this and additional works at: <http://lib.dr.iastate.edu/etd>

 Part of the [Mechanical Engineering Commons](#)

Recommended Citation

Mousa, Saeed, "Roll bonding of metal-polymer-metal sandwich composites" (2017). *Graduate Theses and Dissertations*. 15384.
<http://lib.dr.iastate.edu/etd/15384>

This Dissertation is brought to you for free and open access by the Iowa State University Capstones, Theses and Dissertations at Iowa State University Digital Repository. It has been accepted for inclusion in Graduate Theses and Dissertations by an authorized administrator of Iowa State University Digital Repository. For more information, please contact digirep@iastate.edu.

Roll bonding of metal-polymer-metal sandwich composites

by

Saeed Mousa

A dissertation submitted to the graduate faculty
in partial fulfillment of the requirements for the degree of

DOCTOR OF PHILOSOPHY

Major: Mechanical Engineering

Program of Study Committee:
Gap-Yong Kim, Major Professor
Pranav Shrotriya
Alan Russell
Sriram Sundararajan
Ganesh Balasubramanian

Iowa State University

Ames, Iowa

2017

Copyright © Saeed Mousa, 2017. All rights reserved.

TABLE OF CONTENTS

LIST OF FIGURES.....	v
LIST OF TABLES.....	viii
ACKNOWLEDGMENTS.....	ix
ABSTRACT.....	x
CHAPTER 1 INTRODUCTION.....	1
1.1 Motivation	1
1.2 Research framework and objectives.....	2
1.2.1 Background and state-of-the-art literature review	2
1.2.2 Experimental study on direct adhesion warm roll-bonding metal-polymer-metal multilayer composites	2
1.2.3 Roll bonding of glass fiber reinforced metal-polymer-metal sandwich composites	3
1.3 Dissertation organization.....	3
CHAPTER 2 BACKGROUND AND STATE-OF-THE-ART LITERATURE REVIEW	5
2.1 Direct injection molding technique	8
2.2 Overmolding technique	9
2.3 Heat press technique.....	10
2.4 Roll bonding technique	11
CHAPTER 3 EXPERIMENTAL STUDY ON DIRECT ADHESION WARM ROLL-BONDING METAL-POLYMER-METAL MULTILAYER COMPOSITES	16
3.1 Introduction	16
3.2 Experimental procedure	17
3.2.1 Material preparation and fabrication for T-peel test.....	17

3.2.2	Material preparation and fabrication for small punch test	21
3.3	Results and discussion.....	23
3.3.1	T-peel test results	23
3.3.1.1	Effect of surface roughness on adhesion strength.....	23
3.3.1.2	Effect of preheating temperature on adhesion strength.....	27
3.3.1.3	Effect of rolling speed on adhesion strength.....	29
3.3.1.4	Effect of thickness reduction on adhesion strength.....	33
3.3.2	Small punch test results	35
3.3.2.1	Small punch test	35
3.3.2.2	Fracture analysis.....	40
3.4	Conclusions	46
CHAPTER 4 ROLL-BONDING OF GLASS FIBER REINFORCED METAL-POLYMER- METAL SANDWICH COMPOSITES		48
4.1	Introduction	48
4.2	Experimental procedure	49
4.3	Results and discussion.....	54
4.3.1	T-peel test and single lap shear test	54
4.3.2	Small punch test.....	56
4.3.3	Observation of failure pattern	59
4.4	Conclusions	61
CHAPTER 5 SUMMARY AND SCIENTIFIC CONTRIBUTIONS		63
5.1	Summary	63
5.1.1	Experimental study on direct adhesion warm roll-bonding metal-polymer-metal multilayer composites	63

5.1.2	Roll bonding of glass fiber reinforced metal-polymer-metal sandwich composites	64
5.2	Scientific contributions	65
5.3	Recommendations for the future work	65
BIBLIOGRAPHY		67

LIST OF FIGURES

Fig. 1: Schematic of ULSAB (Lukaschkin et al., 1997).....	7
Fig. 2: Aluminum polypropylene sandwich sheets "Hylite" (Burchitz et al., 2005).	8
Fig. 3: Composite manufactured by direct-injection molding process (Grujicic, 2014).	9
Fig. 4: Example of overmolding process (Grujicic, 2014).	10
Fig. 5: Heat pressing process of metal-polymer-metal sandwich composites (Palkowski and Lange, 2005).	11
Fig. 6: Schematic of indirect adhesion roll bonding of metal-polymer-metal sandwich composites (Sokolova et al., 2010).	12
Fig. 7: Schematic illustration of the warm roll bonding process.	19
Fig. 8: Laboratory rolling mill.	19
Fig. 9: Schematic illustration of the peel test.	20
Fig. 10: The load versus displacement curve of a peel test.	20
Fig. 11: The small punch test (a) SPT setup. (b) Cross sectional view of the SPT.	22
Fig. 12: Optical microscopic images (left) and the corresponding 3D surface profiles (right) of the AL1100 roughened with different sandpaper grit sizes: (A) as-received AL1100 ($R_a=0.6 \mu\text{m}$), (B) grit 80 ($R_a=3.75 \mu\text{m}$), (C) grit 50 ($R_a=5.63 \mu\text{m}$), and (D) grit 36 ($R_a=8.31 \mu\text{m}$).....	24
Fig. 13: Peel strength of AL1100-PU-AL1100 fabricated with different surface roughness values. Data: Mean \pm SD (n=3).	25
Fig. 14: Fracture surfaces of AL1100/PU after peel test with 60% reduction, 200°C preheating, and 30 rpm rolling speed for different surface roughness values: (A) as-received AL1100 ($R_a=0.6 \mu\text{m}$), (B) sandpaper grit 80 ($R_a=3.75 \mu\text{m}$), (C) sandpaper grit 50 ($R_a=5.63 \mu\text{m}$), and (D) sandpaper grit 36 ($R_a= 8.31 \mu\text{m}$).....	27
Fig. 15: Variation in peel strength of AL1100-PU-AL1100 versus preheat temperature. Data: Mean \pm SD (n=3).	29

Fig. 16: Variation in peel strength of Al 1100/PU/AL1100 versus rolling speed. Data: Mean \pm SD (n=3).	30
Fig. 17: Schematic diagram of optimum rolling speed.....	31
Fig. 18: DOE study results. (A) Prediction profiles of preheat temperature and rolling speed. (B) Interaction plot of preheat temperature and rolling speed parameters.	33
Fig. 19: Variation in peel strength of AL1100-PU-AL1100 versus thickness reduction. Data: Mean \pm SD (n=3).	34
Fig. 20: Cross sectional of AL1100-PU-AL1100 sample with 60% thickness reduction.	35
Fig. 21: Typical load displacement curve of AL1100-PU-AL1100 SPT sample.....	36
Fig. 22: Ultimate load versus different thickness reductions. Data: Average (n=3).....	37
Fig. 23: Specific load for different thickness reductions. Data: average (n=3).	38
Fig. 24: Average stiffness for different thickness reductions. Data: Average (n=3).	39
Fig. 25: Specific fracture energy for SPT with various thickness reductions. Data: Average (n=3).....	40
Fig. 26: Cross sectional images of fractured samples of SPT for different thickness reductions: (a) 40% (AL-PU-AL), (b) 50% (AL-PU-AL), (c) 60% (AL-PU-AL), (d) 75% (AL-PU-AL), (e) 50% (AL monolayer), and (f) 75% (AL monolayer).	43
Fig. 27: Load versus displacement curves for AL1100-PU-AL1100 sandwich composites and AL1100 samples for thickness reduction of 75%.	44
Fig. 28: Cross sectional images for the 75% thickness reduction of AL1100-PU-AL1100 sandwich composites at different SPT loads: (a) 200 N, (b) 500 N, (c) 700 N, and (d) 800 N....	45
Fig. 29: S-glass fibers before and after ball milling for 30 seconds.	51
Fig. 30: A schematic illustration of fabricating fiber-reinforced, roll-bonding of metal-polymer composites.....	52
Fig. 32: (a) Sample geometry of the shear test, and (b) The load versus displacement of a shear test.	53

Fig. 34: Peel strength measurements of the samples with and without reinforcement at reductions thickness of 60% and 75%. Mean \pm SD (n=3).....	55
Fig. 35: Shear strength measurements of the samples with and without reinforcement at reduction thicknesses of 60% and 75%. Mean \pm SD (n=3).....	56
Fig. 36: Ultimate load measurements at reduction thicknesses of 60% and 75% of the samples of AL monolayer, samples of sandwich composites with and without reinforcement. Mean \pm SD (n=3).....	57
Fig. 37: Specific load measurements at reduction thicknesses of 60% and 75% of the samples of AL monolayer, samples of sandwich composites with and without reinforcement. Mean \pm SD (n=3).....	58
Fig. 38: Specific fracture energy measurements at reduction thicknesses of 60% and 75% of the samples of AL monolayer, samples of sandwich composites with and without reinforcement. Mean \pm SD (n=3).....	59
Fig. 39: SEM images of shear failure surfaces with glass-fiber reinforcement: (a) peeled-off and debonding marks of glass fiber, (b) fiber bridging and fracture observation, (c) fiber breaking and peeled off marks, and (d) fiber free end.....	61

LIST OF TABLES

Table 1: Summary of formability studies of metal-polymer sandwich composites.	14
Table 2: Specification of AL1100 strip and PU sheet.	18
Table 3: WRB process parameters and their settings.	18
Table 4: Density and final thickness for the AL1100-PU-AL1100 sandwich composites at various thickness reductions.	22
Table 5: Contact times of different rolling speeds.	31
Table 6: The settings and results of design of experiments.	32
Table 7: Thickness measurements at different SPT loads.	45
Table 8: Specification of AL1100 strip, PU sheet, and glass fiber.	50

ACKNOWLEDGEMENTS

First of all, I would like to express my gratitude to everyone involved in any of the projects that make this dissertation. I would like to thank my major professor, Prof. Gap-Yong Kim, for the opportunity to work with him. He has offered his support through his knowledge, expertise, and time. The success of my research would not have been possible without his professional experience and support. I would like to extend my appreciation to Prof. Shrotriya, Prof. Russell, Prof. Sundararajan, and Prof. Balasubramanian for their time being part of my dissertation committee, their valuable discussion, and inspiring comments over the evaluation process.

I also would like to send special thanks to my family: my parents, my loving wife, and my kids. They have provided the love and support I needed to pass through my difficult times. This dissertation is proof of their support.

Finally, I would like to acknowledge the scholarship support provided by Jazan University-Saudi Arabia under Contract no. (35/7/20739).

ABSTRACT

Metal-polymer sandwich composites have been rapidly replacing metallic materials in the aerospace and automobile industries. Their desirable mechanical properties, including excellent fatigue and impact strength, as well as damage tolerance, are accomplished without sacrificing the benefit of lightweight. Manufacturing metal-polymer sandwich composites via roll bonding can offer great advantages over other techniques such as overmolding and injection molding, which are more complex and costly. Roll bonding of multilayer composites, however, is challenging because of the significant differences in the mechanical properties and the adhesion characteristics of polymeric and metallic materials. In this study, a three-layer metal-polymer-metal sandwich composite, which consisted of aluminum (AL1100) and polyurethane (PU), was successfully fabricated using a direct adhesion warm roll bonding (WRB) technique without the use of an adhesive agent. In the first part of this work, the effects of WRB process parameters, which include surface roughness, preheat temperature, rolling speed, and total thickness reduction, on the adhesion strength have been investigated using the peel test. Mechanical interlocking was the primary adhesion mechanism in direct bonding of the aluminum and polyurethane. The failure mode transitioned from adhesive to cohesive as the surface roughness increased. The optimum rolling speed and preheat temperature of the WRB process were identified. In the second part of this work, the small punch test (SPT) was employed to characterize the mechanical properties of the sandwich composites, including ultimate load, specific load, average stiffness, and specific fracture energy, at various thickness reductions. The results showed significant improvements in the specific fracture energy of the sandwich composites compared with monolithic material by 26%, 20%, and 36% at thickness reductions of 50%, 60%, and 75%, respectively. The presence of the soft layer in the sandwich composite

helps to arrest cracking propagation. In the third part, glass fiber introduced at the interface of metal-polymer-metal laminated composites using the WRB process. The reinforcing effects of the glass fiber on the adhesion strength and shear resistance were analyzed. A single lap shear test, SPT, and T-peel test were used to evaluate the mechanical and bonding properties, and electron microscopy was employed to analyze the fracture behavior of the fiber-reinforced laminate composites. The shear strength of the glass fiber reinforced sandwich composite improved nearly 40% compared with the unreinforced samples. The SPT results showed increase in the ultimate load, specific load, and specific fracture energy for the samples with glass fibers incorporated between the roll-bonded layers.

CHAPTER 1 INTRODUCTION

1.1 Motivation

Structural weight reduction is one of the main design objectives in the aerospace and automotive industries. Among the various materials developed, sandwich composites, which comprise two skin sheets and a low-density core material, have shown a promising potential for weight reduction applications (Kopp et al., 2005). Compared with homogenous metallic sheets, metal-polymer-metal sandwich composites offer lower density while maintaining bending rigidity almost equal to that of a monolithic metallic sheet of the same thickness. Metal-polymer-metal sandwich composites have been used in many industries including the automotive industry, household appliance manufacturing, as well as in home and garden applications (Ruokolainen and Sigler, 2008a).

Various manufacturing techniques have been applied to manufacture metal-polymer-metal sandwich composites including overmolding (Joachim Gähde, 1992), direct injection molding (Ramani and Moriarty, 1998), heat pressing (Kim et al., 2003), and roll bonding (Palkowski and Lange, 2005). In most of these techniques, metal-polymer-metal sandwich composites can be fabricated either with a glue agent (indirect adhesion) or without a glue agent (direct adhesion) to produce bonding between the laminates. Among these processes, roll bonding offers the advantages of continuous production and cost reduction over other techniques. Most of the studies that examined the roll bonding of metal-polymer sandwich composites employed an indirect adhesion technique using a glue agent between the layers.

In this study, a newly developed direct adhesion technique using a warm roll-bonding (WRB) process was used to manufacture metal-polymer-metal sandwich composites. The effect

of the WRB process parameters on the adhesion strength and mechanical properties of the manufactured metal-polymer-metal sandwich composites were investigated. In addition, a new technique is introduced to fabricate fiber-reinforced, roll-bonded metal-polymer sandwich composites for enhanced adhesion and shear performance. Glass fibers were introduced at the interface between the metal skins and the polymer core using the WRB process. The effects of reinforcing glass fibers on the mechanical and bonding properties were investigated by performing T-peel test, single lap shear test, and small punch test (SPT) as well as electron microscopy analysis. The results will provide and facilitate the use of the direct adhesion warm roll-bonding technique to produce metal-polymer-metal sandwich composites panels.

1.2 Research framework and objectives

1.2.1 Background and state-of-the-art literature review

In this chapter, a comprehensive overview of the key aspects of composite manufacturing technologies used to manufacture metal-polymer sandwich composites is provided. Specifically, the following manufacturing technologies are discussed: (a) direct injection molding; (b) overmolding; (c) heat pressing; and (d) roll bonding.

1.2.2 Experimental study on direct adhesion warm roll-bonding of metal-polymer-metal multilayer composites

Roll bonding of multilayer composites is challenging because of significant differences in the mechanical properties and adhesion characteristics of polymeric and metallic materials. The first objective of this study was to introduce a novel manufacturing technique to produce metal-polymer-metal sandwich composites without using a glue agent between the layers (direct adhesion warm roll-bonding). The effect of the direct adhesion warm roll-bonding process parameters on the resultant adhesion strength were investigated. The WRB process parameters

include surface roughness, preheating temperature, rolling speed, and thickness reduction ratio. In addition, a small punch test (SPT) was employed to characterize the mechanical properties of the of the manufactured sandwich composites, which include ultimate load, specific load, average stiffness, and specific fracture energy, at different thickness reductions. The mechanical properties of the sandwich composites were compared with the metal materials at the same thickness.

1.2.3 Roll bonding of glass fiber reinforced metal-polymer-metal sandwich composites

Many fiber-reinforced laminate composites offer a combination of strength and modulus that are either comparable to, or better than, many traditional metallic materials. Because of their low density, the strength-weight ratios and modulus-weight ratios of these composite materials are markedly superior to those of metallic materials. In this chapter, a new technique is introduced to fabricate fiber-reinforced, roll-bonded metal-polymer sandwich composites for enhanced adhesion and shear performance. The glass fibers were introduced at the interfaces between the metal skins and the polymer core and underwent WRB process. The effects of reinforcing glass fibers on the mechanical and bonding properties were investigated by performing T-peel test, single lap shear test, and small punch test (SPT) as well as electron microscopy analysis.

1.3 Dissertation organization

The remainder of this thesis is divided into four chapters. In Chapter 2, a literature review on the state-of-the-art the metal-polymer-metal sandwich composites and common manufacturing techniques is presented. In Chapter 3, a metal-polymer-metal sandwich composite was manufactured using a direct adhesion technique after which its adhesion and mechanical characterizations were investigated. Chapter 4 presents the results of reinforcing

glass fibers into metal-polymer-metal composites during roll bonding. A summary and contributions of this research are presented in Chapter 5.

CHAPTER 2 BACKGROUND AND STATE-OF-THE-ART LITERATURE REVIEW

Sandwich is a common principle in nature and hence the concept is older than mankind itself (Herrmann et al., 2005). The branches of the elder tree are a good example for soft core sandwich structure. The boons in the skeletons of animals and humans are sandwich structures with foam like core materials as well. Natural sandwich structures are subjected to complex load cases. The bones in legs have to withstand repetitive, super positioned bending and compression loads. Moreover nature imposes a strict demand for lightweight primary structure. All the mentioned examples show the principle of structural optimization: minimum use of material for maximum performance (Thomsen et al., 2006).

The first sandwich material to be used in industry dates back to 1924, when a wooden sandwich material consisting of plywood and balsa was used in aircraft. The rapid development of the aircraft industry and the demand for lightweight, stiff, and strong materials led to the widespread development of various sandwich materials (Ziegmann, 1998). In 1987, an advanced sandwich material known as Glass Laminated Aluminum Reinforced Epoxy (GLARE) was patented by Akzo Nobel. This sandwich material offers better damage tolerance behavior, excellent corrosion and fire resistance, all with a low specific weight. Several other advanced sandwich materials based on aluminum were developed in the same period including Aramid Aluminum Laminates (ARALL) and Carbon Fiber Reinforced Aluminum Laminates (CARALL) (Kawai and Hachinohe, 2002).

The metal-polymer-metal sandwich composite, which consists of two metal skins with a polymer core in between, is a representative of such materials showing high stiffness and strength, good formability as well as high plasticity, high damping and vibration capacity of light polymer material. Sandwich composites of metal-polymer-metal are increasingly finding their

way into the automobile industry (Yang et al., 2001). They are used for car bodies because of their lightweight, and for sound reduction. Sandwich materials are used with either a homogenous or inhomogeneous core of foams or other hard materials. Examples of components of sandwich constructions are gearbox covers, hoods, car trunk covers, and chassis frame components (Link, 2001). A well-known example for the use of sandwich sheet metals in the automobile industry is the lightweight construction bodywork Ultra-Light Steel Auto Body (ULSAB). Some of the components, such as the spare wheel hollow and cowl application were manufactured of steel sandwich sheets. These components can be up to 50% lighter than a comparable sheet of homogenous steel, all without compromising performance. The material consists of two thin steel sheets, which are bonded with thin polypropylene material layers as core material as shown in Fig. 1. The polymer core acts as a spacer between the two outer sheets, separating the outer surfaces from the neutral axis when a bending load is applied. ULSAB possesses many of the same processing possibilities such as deep drawing, shear cutting, laser cutting, drilling, adhesive bonding and riveting, with steel sheets; however, it cannot be welded (Palkowski and Lange, 2005).

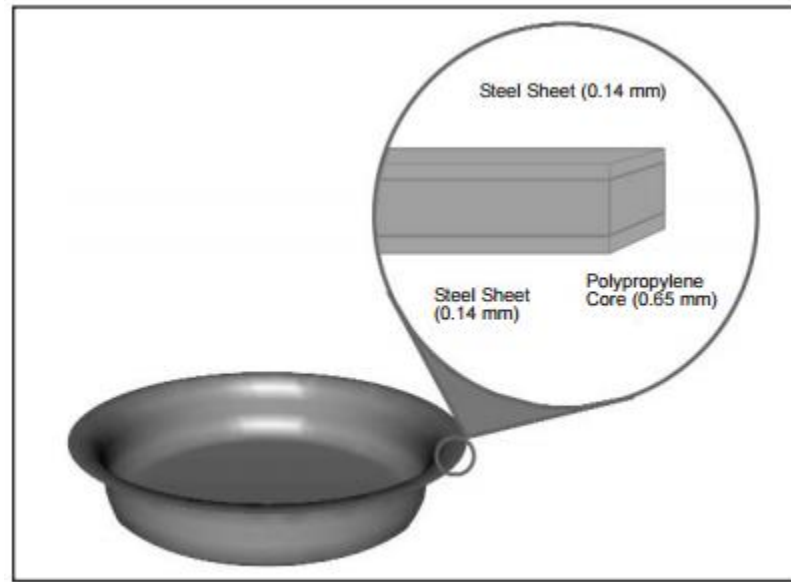


Fig. 1: Schematic of ULSAB (Lukaschkin et al., 1997).

Aluminum polypropylene sandwich sheets called “Hylite” were used for the roof and the hood of a Ford E-Ka, in May 2000. The E-Ka developed in the Ford research center “Aix-la-Chapelle” offers several lightweight construction elements. The weight of the E-Ka could altogether be reduced by 45 kg, with the use of aluminum. The roof (weigh savings: 5.5 kg) and the hood (weight savings: 5.3 kg) were made of Hylite, which is composed of two layers of aluminum enclosing a layer of polypropylene in a sandwich manner as shown in Fig. 2. The polymer core material is beneficial not only because of the significant weight that is saved when compared to the corresponding metal components without any loss of strength or stiffness, but also for the enhancement of specific mechanical properties, including vibration damping, impact response, thermal insulation property, and acoustic damping (Burchitz et al., 2005).



Fig. 2: Aluminum polypropylene sandwich sheets "Hylite" (Burchitz et al., 2005).

Major manufacturing techniques of metal-polymer-metal sandwich composites that are currently employed in the automotive and non-automotive industries include: (a) direct injection molding; (b) overmolding; (c) heat pressing; and (d) roll bonding. Each of these techniques is introduced below.

2.1 Direct injection molding technique

This process was originally introduced and patented by Johannaber et al. (1983). In general, the process involves the following steps as shown in Fig. 3: (a) sheet metal blanks are stamped to obtain the desired shape of the metal inserts; (b) flared through holes are punched into the metal inserts; (c) inserts are next placed in the injection molding die; and (d) injection molding is used to overmold the metal inserts with a cross-ribbed integrated structure. In this process, tight interlocking between the metal insert and the polymer cross ribbed structure helps hold the whole structure together. Direct injection molding has a variety of advantages including enhanced stability of final product dimensions, weight and material savings, and the potential to produce a component with low internal stress and deformation (Bryce, 1996). One of the disadvantage is that the mechanical values are generally lower than components made using

other techniques with the same dimensions, and streaking can be visible on the component surface (Moriwaki, 1996). Many metal-polymer-metal sandwich composites used the same technique with different material combinations, including AA6061-T6/polycarbonate and 1018 steel/polycarbonate sandwich composites (Honkanen, 2011). This process can be used with or without a glue agent between the layers.

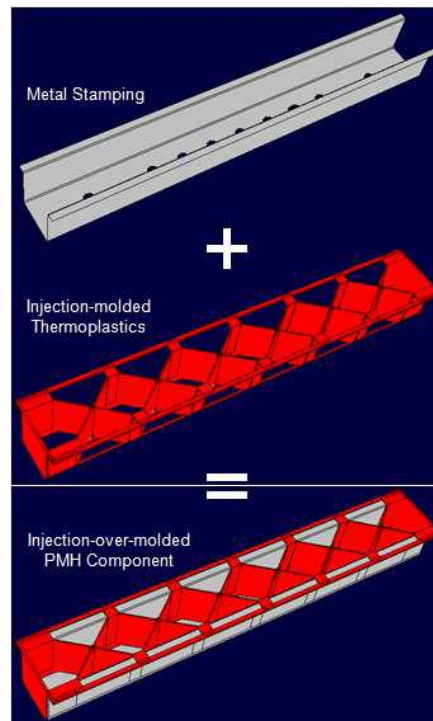


Fig. 3: Composite manufactured by direct-injection molding process (Grujicic, 2014).

2.2 Overmolding technique

Overmolding is the process of adding an additional layer of material over an already existing layer. In this process, one material, usually a polymer, is molded onto a second metal material. The overmolding process can be used to enhance many features of product design, including safety, ergonomics, and product functionality (Rowley, 2001). The challenge in the overmolding process is achieving maximum adhesion between the polymer and the metal, and

that can be achieved by molecular adhesion, and mechanical interlocks. This technique was originally developed and patented by Zoellner and Evans (2002) and employed for the front-end module of a 2004 light truck intended for the South American market. The manufacturing process involves the following main steps: (a) a U-shaped steel stamping is placed in an injection molding; and (b) the polymer is overmolded to the U-shape steel. The main benefits of this process is that it can be used for fabricating any closed structure, including sections with hollows. Various metal-polymer sandwich composites with different materials combinations have been fabricated using this process including AA2024-O/polypropylene, and 2024-T3/polypropylene sandwich composites (Gresham et al., 2006). This process can be employed with or without a glue agent. A schematic of the technique is shown in Fig. 4.

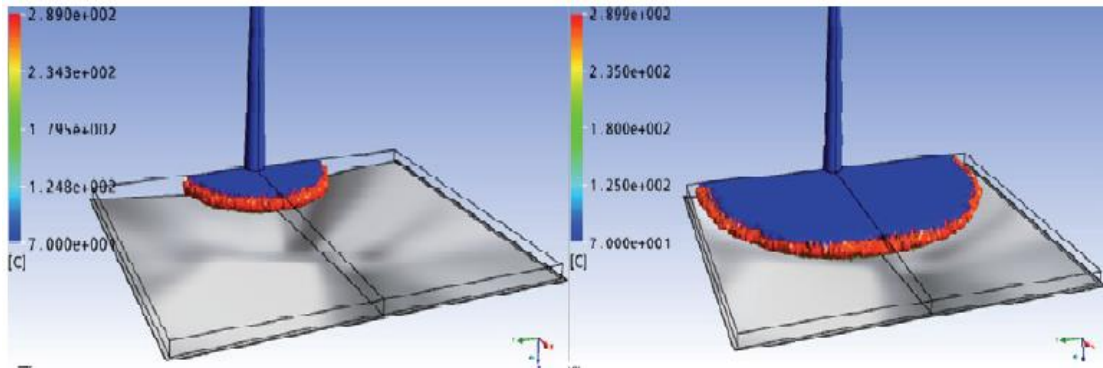


Fig. 4: Example of overmolding process (Grujicic, 2014).

2.3 Heat press technique

This process used to manufacture metal-polymer-metal sandwich composites by applying the heat and pressure at the same time (Winandy and Kamke, 2004). The sample size depends on the press size as shown in Fig. 5. Many aspects are involved in this process, from resin curing and bonding time, to controlling the heat and pressure during the pressing; these constraints limit the deployment of this process in the automotive industry.

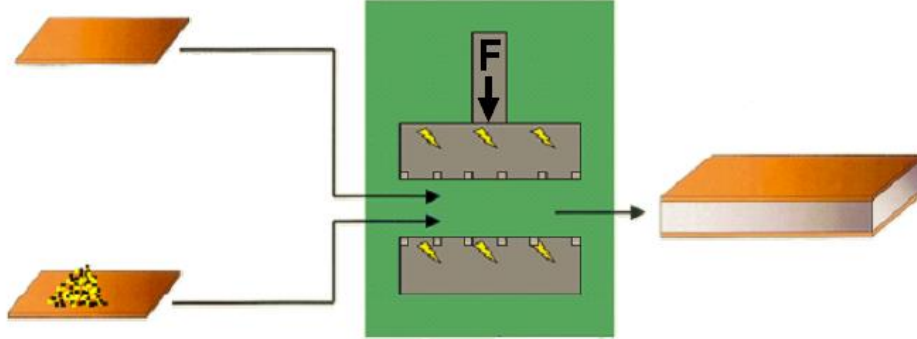


Fig. 5: Heat pressing process of metal-polymer-metal sandwich composites (Palkowski and Lange, 2005).

2.4 Roll bonding technique

Layered alloys and composites have attracted increasing attention for industrial applications. Among all of the technologies, the roll bonding (RB) process for producing layered sheets and foils has witnessed rapid growth and development in recent years due to its unique service performance features when compared with other methods (Pan et al., 1989). The RB process is very simple and can easily be automated. Indeed, RB is a solid phase welding process, whereby the bonding is established by joint plastic deformation of the metals that are to be bonded (Lukaschkin et al., 1997). Bonding is obtained when the surface expansion exposes the surfaces of the virgin metal or when the pressure reaches a value large enough to extrude the virgin material through the cracks of the fractured layer, which results in the establishment of contact and bonding between opposing virgin surfaces. The solid state joining technique in RB can be applied to a large number of materials, including two layers of the same material, thus possessing identical attributes, or the layers may be different materials, thus possessing widely varying mechanical and metallurgical properties (Jamaati and Toroghinejad, 2011).

Roll bonding of metal-polymer sandwich composites can offer great advantages over other techniques, because the other techniques are more complex and costly due to the equipment involved and required mold design. Most of roll bonding studies of metal-polymer-metal sandwich composites were performed by a research group at the (Institute of Metallurgy (IMET)) in Germany. The novel process that IMET developed to manufacture steel-polypropylene-steel sandwich composites involves the following steps as shown in Fig. 6: (a) the metal sheets were cleaned and degreased; (b) the metal sheet was coated with defined layer of adhesive (epoxy resin); (c) the first sheet metal was joined to a polypropylene foil in a rolling process; and (d) the produced sandwich was joined to the second steel sheet. Carrado. et al. (2010) produced steel-polypropylene-steel sandwich composites using this roll bonding technique and employed a glue agent between the composite layers. They investigated the forming behavior of the composites, and found it to be close to that of mono-material.

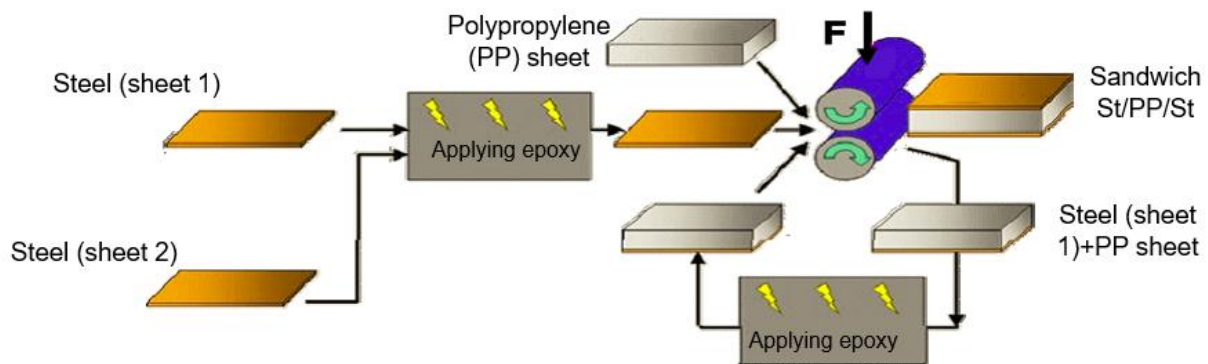


Fig. 6: Schematic of indirect adhesive roll bonding of metal-polymer-metal sandwich composites (Sokolova et al., 2010).

It is well established that the structural and functional performance of the metal-polymer-metal sandwich composites depend on the extent of the load transfer that takes place through the polymer-metal interfaces, and this, in turn, is controlled by the mechanism and strength of the

metal-to-polymer bonding. Hence, it is important to identify the difference between direct and indirect adhesion. Direct adhesion relies on the formation of surface roughness length-scale metal-polymer mechanical interlocking, which is formed as a result of the infiltration of the surface roughness features on the metal substrate by the subsequent solidification of the molten polymer. On the other hand, in the case of the indirect adhesion employs metal surface priming, or the use of an adhesive between the bonded layers of meta-polymer (Grujicic, 2014).

In the automotive industry, 90% of the deformation of the blank is usually performed during the initial stamping operation; therefore this process has the highest impact on part quality. This initial operation is usually dominated by the formability of the blank into the die cavity. To obtain successful high production of metal-polymer sandwich composites using stamp forming, an understanding of the formability behavior is essential (Gresham et al., 2006). Because of that reason, many studies of the formability of the metal-polymer sandwich composites manufactured with different manufacturing techniques were investigated. Both experimental and theoretical investigations on formability of the metal-polymer sandwich composites have been undertaken by several authors as summarized in Table 1. Most of metal-polymer sandwich composites reached values comparable to those of monolithic sheets; in tensile tests; they followed the rule of mixtures. Moreover, they attained better forming values compared to the monolithic materials with benefits of lightweight savings. It can be stated that the polymer materials in sandwich composites can have a significant positive impact on the formability when compared to the skin metal sheets.

Table 1: Summary of formability studies of metal-polymer sandwich composites.

Manufacturing technique	Skin material	Core material	Direct/indirect adhesion	Author(s)
Heat pressing	AL2024-O	Polypropylene	Direct	(Gresham et al., 2006)
	AL6061-T4	Glass-fiber reinforced polypropylene	Direct	(Gresham et al., 2006; Prolongo et al., 2006)
	AL2024-T3	Glass-fiber reinforced polypropylene	Direct	(Prolongo et al., 2006)
	Low carbon steel	PolyVinyl Chloride (PVS)	Indirect	(Karlsson and TomasÅström, 1997)
	AA3150	Polyethylene	Indirect	(Kim et al., 2009)
	AA5052	Polyethylene	Indirect	(Kim et al., 2003)
Overmolding	AA2024-T3	Polypropylene	Direct	(Ramani and Moriarty, 1998)
	Steel ST38	Polyurethane	Direct	(Sasaki et al., 1998)
	Steel	Polyurethane	Direct	(Ramani and Moriarty, 1998)
Direct injection molding	AA6061-T6	Polycarbonate	Direct	(Joachim Gähde, 1992)
	Steel 1018	Polycarbonate	Direct	(Grujicic, 2014)
	Steel	Polystyrene	Direct	(Reyes and Kang, 2007)
Roll bonding	Steel 316L	PP-PE	Indirect	(Carradò et al., 2011)
	Steel TS245	Polyolefin	Indirect	(Sokolova et al., 2010)
	Titanium	PP-PE	Indirect	(Harhash et al., 2014)

The literature survey shows that all roll bonding studies of metal-polymer sandwich composites were using a glue agent between the layers (indirect adhesion technique), which increases the number of manufacturing steps, and which affected the cost and the quality of the

final component. In addition, the glue agent such as, epoxy became hard and brittle after curing, and that change directly affected the formability of the manufactured composites as investigated by Ruokolainen and Sigler (2008b). Those studies, however, were more focused on the formability of the material combination rather than the adhesion between layers (Carradò et al., 2011a). In addition, various approaches have been investigated to enhance the formability and the shear strengths of the roll-bonded metal-polymer-metal sandwich composites. Carradò et al. (2011b) used various surface treatments (corona discharge and plasma treatment) on the metal surface to increase the wettability and found that the shear strength and the formability of the indirect roll bonded composites increased when compared to the untreated samples. Sokolova et al. (2011) used embedded solid and mesh steel inlays between the steel-polymer sandwich composite layers to improve the adhesion performance, and a slight improvement was achieved while formability improved by 9% due to the mesh inlays.

In this thesis, a direct adhesion warm roll-bonding technique (WRB) was introduced to fabricate metal-polymer-metal sandwich composites, without the use of direct heat for fusion or adhesives, and that was the first main part of this thesis. The new bonding mechanism introduced by WRB has improved the mechanical properties and therefore eliminates the use of adhesives. In the second part of this thesis, a new technique is introduced to fabricate fiber-reinforced, roll bonded metal-polymer sandwich composites for enhanced adhesion and shear performance. The WRB will expand the capabilities of the traditional roll bonding process, typically limited to metal-to-metal bonding, to metal-to-polymer sandwich composites. The following chapters will present the WRB of unreinforced and reinforced metal-polymer sandwich composites, and their mechanical properties.

CHAPTER 3 EXPERIMENTAL STUDY ON DIRECT ADHESION WARM ROLL-BONDING METAL-POLYMER-METAL MULTILAYER COMPOSITES

3.1 Introduction

Manufacturing of metal-polymer sandwich composites via roll bonding can offer a great advantage over other techniques such as overmolding and injection molding, which are more complex and costly due to the equipment involved and mold design. Most of studies found on roll bonding of metal-polymer sandwich composites were performed by a research group at the Institute of Metallurgy (IMET) in Germany (Institute of Metallurgy (IMET)). Carrado. et al. (2010) produced a three layer sandwich sheet by roll bonding. They investigated the forming behavior of the composites, and found it to be close to the mono-material. Moreover, the formability of the roll bonded composites were more favorable than that of the composites made by the heat press technique (Carradò et al., 2011a).

Roll bonding of these composites is challenging due to the large difference in mechanical properties and adhesion characteristics of polymeric and metallic materials. The previous roll bonding studies on metal/polymer sandwich composites were more focused on the formability of material combinations rather than the adhesion between the layers (Carrado. et al., 2010), and most of them employed an indirect adhesion technique using a glue agent between the layers (Carradò et al., 2011a). No detailed studies were found that investigated the influence of roll bonding parameters on the adhesion strength and mechanical properties of metal-polymer-metal sandwich composite by a direct adhesion method.

In the first part of this work, AL1100-PU-AL1100 sandwich composite was fabricated by a warm roll bonding (WRB) at elevated temperatures to understand the relationship between the

WRB process parameters and the resultant adhesion strength. The WRB process parameters included surface roughness, preheat temperature, rolling speed, and thickness reduction. In the second part of this work, a small punch test (SPT) was employed to characterize the mechanical properties of the AL1100-PU-AL1100 sandwich composites, which include ultimate load, specific load, average stiffness, and specific fracture energy, at different thickness reductions. Fracture analysis was conducted to evaluate the fracture behavior of the composite panels.

3.2 Experimental procedure

3.2.1 Material preparation and fabrication for T-peel test

A commercially pure aluminum (AL1100) strip and polyurethane (PU) sheets were used to make the sandwich composite. A thermoplastic PU was selected as the core material since it becomes soft and formable when heated. Such a property makes it easy to flow through the rough surfaces of the metal substrate during roll bonding. In addition, thermoplastic PU has high tear strength (50 kN/m) compared with most of other plastics in a similar hardness range (medium hard plastics) (Watabe et al., 1977), which make it an excellent candidate for the current study. The AL strips were cut into dimensions of 70 mm × 20 mm × 0.5 mm, and the PU sheets were cut into dimensions of 60 mm × 20 mm × 0.8 mm. The specification of AL1100 strips and PU sheets are summarized in Table 2. In order to produce a satisfactory bond in WRB, it is important to remove the contaminated layers on the surfaces of the strips. The sample surfaces were first degreased with ethanol, followed by sanding of the surface. Sandpapers with three different average grit sizes of 36, 50, and 80 were used to investigate the effect of surface roughness on the bond strength. Surface roughness values were measured by a 3D profilometer (Zygo, NewView 7100). The bonding took place immediately after degreasing

and sanding to avoid surface oxidation. The process parameters and their settings are shown in Table 3.

Table 2: Specification of AL1100 strip and PU sheet.

Material	Chemical composition (wt.%)	Tensile Strength (MPa)	Yield Strength (MPa)	Elongation (%)	Density (g/cm³)
AL1100	99.61 Al, 0.11 Si, 0.55 Fe, 0.11 Cu, and 0.07 others	85	33	30	2.7

Material	Shore Durometer (ASTM D2240-64T)	Compression Set (ASTM D395-61, Method B) 22 Hrs. @ 158 F	Ultimate Tensile Strength (ASTM D412-61T)	Density (g/cm³)
PU	60 A (medium hard)	30% Max	21 MPa	0.85

Table 3: WRB process parameters and their settings.

Parameters	Values
Surface roughness (grit)	AL1100 as-received, 80, 50, and 36
Preheat temperature (°C)	170, 190, 200, and 240
Rolling speed (rpm)	18, 24, 30, 40, 50, and 60
Thickness reduction (%)	40, 50, 60, and 75

A schematic of the WRB process employed in our study is described in Fig. 7. The preheating of AL1100 samples was accomplished using a furnace at different temperatures for 15 min. Then, each sample was assembled by inserting the PU sheet between the two AL1100

strips. The samples were joined by a rolling mill (Durston-DRM 130) with a roll diameter of 65 mm as shown in Fig. 8.

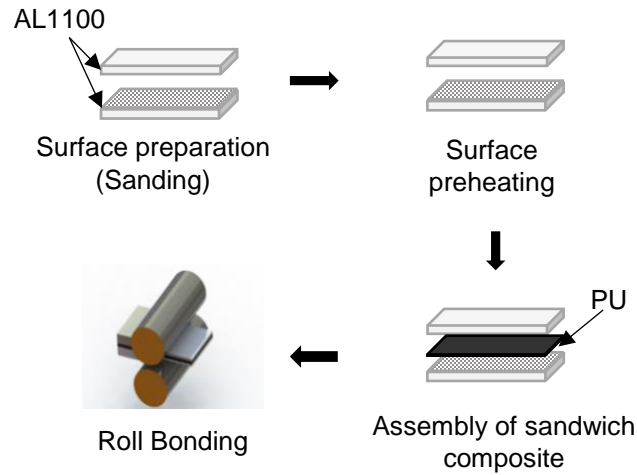


Fig. 7: Schematic illustration of the warm roll bonding process.



Fig. 8: Laboratory rolling mill.

The adhesion between the core and the metal sheets was investigated by T (180°) peel test according to the DIN53282 using the setup shown in Fig. 9 (DIN53281, 1979). The peel test was performed using a universal testing machine (TestResources Inc.) with a crosshead

speed of 20 mm/min. A typical force response from the peel test is shown in Fig. 10 where the average load is noted. The average peel strength can be calculated by:

$$\text{Average peel strength} = \frac{\text{average load (N)}}{\text{bond width (mm)}} \quad (1)$$

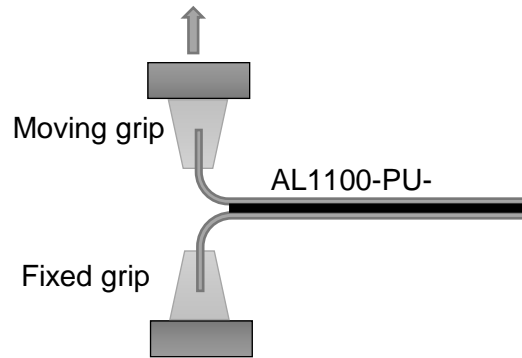


Fig. 9: Schematic illustration of the peel test.

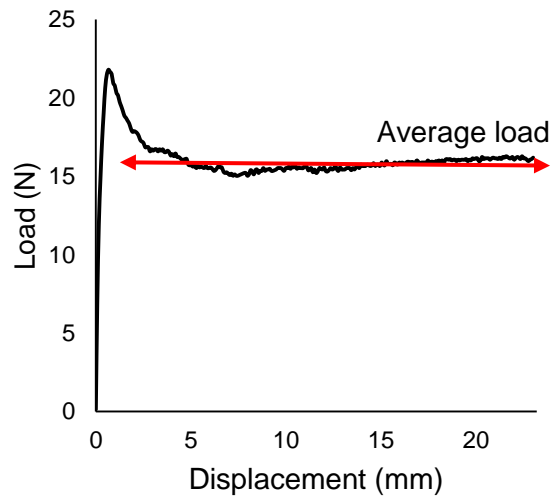


Fig. 10: The load versus displacement curve of a peel test.

3.2.2 Material preparation and fabrication for small punch test

The material preparation for SPT was same as the T-peel test with various thickness reductions (40%, 50%, 60%, and 75%), and fixed parameters for the surface roughness, rolling speed, and preheat temperature. Grit 50 was used for sanding the metal surfaces to generate fresh surface and facilitate the bonding. The rolling speed and preheat temperature were 30 rom, and 200°C, respectively.

A SPT was used to analyze mechanical performance of the sandwich composites since the samples were not large enough for the full size bulge test. A number of mechanical properties can be measured from the SPT such as ultimate load, average stiffness (Tang et al., 2003), fracture energy (Bulloch, 2004), and fracture strain (Isselin and Shoji, 2009). Due to the small size specimen required to perform a SPT, a single sample can provide multiple test specimens (Edidin and Kurtz, 2001).

A universal testing machine (Test Resources) was used for the SPT. The SPT was carried out using an experimental device shown in Fig. 11. The experimental setup included a disc specimen, a 6 mm diameter ceramic ball, and a specimen holder that consisted of an upper and lower die on which the sample was placed and centered on a 10 mm hole. The sample was set between the upper and lower dies, which was tightened with clamping screws. The SPT was conducted at a crosshead speed of 0.2 mm/min with load cell of 5 kN capacity. The values of the load and cross head displacement are recorded simultaneously over time.

In the SPT study section, the sandwich composite samples were rolled with various thickness reductions as summarized in Table 4. The corresponding monolayer AL1100 sheets were prepared by rolling to the same final thicknesses as the composite panels and then annealed at 350°C for 30 min. The composite and monolayer samples were cut into a circular shape with

20 mm diameter for the SPT. The tests were repeated three times for each reduction. Finally, a fracture analysis by optical microscopic was performed to analyze the thinning effect on the sandwich composite panels.

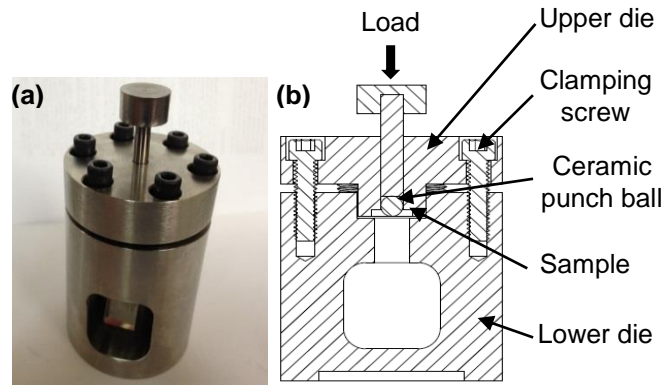


Fig. 11: The small punch test (a) SPT setup. (b) Cross sectional view of the SPT.

Table 4: Density and final thickness for the AL1100-PU-AL1100 sandwich composites at various thickness reductions.

Notation	Total thickness reduction (%)	Total thickness of AL skin (mm)	PU thickness (mm)	Final thickness of AL-PU-AL (mm)	Density of AL-PU-AL (g/cm^3)
A	40	0.65	0.55	1.2	1.87
B	50	0.48	0.44	0.92	1.83
C	60	0.50	0.38	0.88	1.98
D	75	0.55	0.11	0.66	2.29

3.3 Results and discussion

3.3.1 T-peel test results

The effects of surface roughness, preheat temperature, rolling speed, and thickness reduction were analyzed on bond strengths of roll bonded AL1100-PU-AL1100 sandwich composites.

3.3.1.1 Effect of surface roughness on adhesion strength

In order to investigate the effect of surface roughness on adhesion strength, sandpapers with grits of 80, 50, and 36 were used to roughen the AL1100 surfaces. Fig. 12 shows the AL1100 samples with four different surface roughness values. The initial surface roughness of the as-received AL1100 sheet had $R_a = 0.6 \mu\text{m}$. After using sandpaper papers with grits of 80, 50, and 36 the surface roughness values changed to $3.75 \mu\text{m}$, $5.63 \mu\text{m}$, and $8.31 \mu\text{m}$, respectively.

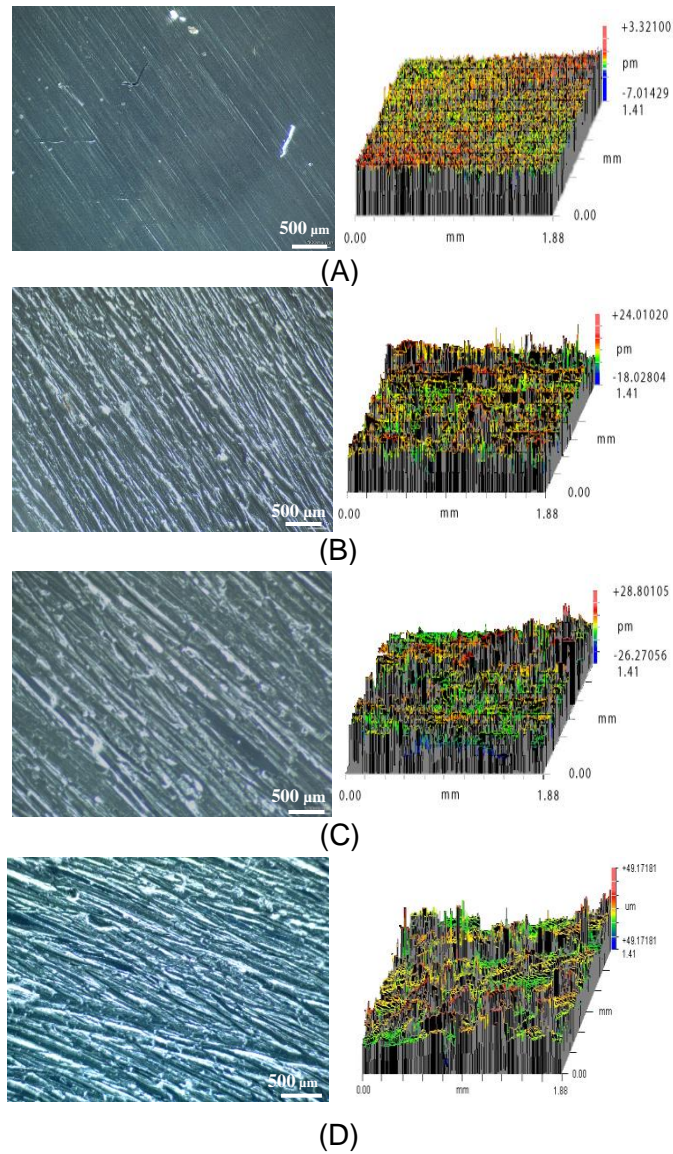


Fig. 12: Optical microscopic images (left) and the corresponding 3D surface profiles (right) of the AL1100 roughened with different sandpaper grit sizes: (A) as-received AL1100 (Ra=0.6 μm), (B) grit 80 (Ra=3.75 μm), (C) grit 50 (Ra=5.63 μm), and (D) grit 36 (Ra=8.31 μm)

Fig. 13 shows the effect of surface roughness on the adhesion strength of AL1100-PU-AL1100. The adhesion strength of sandwich composite with as-received AL1100 was 0.5378

N/mm. Compared with the as-received sample, the bond strengths of samples with $R_a=3.75$, $R_a=5.63 \mu\text{m}$, and $R_a=8.31 \mu\text{m}$ increased by 20%, 50%, and 30%, respectively. The different sandpapers produced surfaces with high asperities and deep valleys, which directly affected the mechanical interlocking at the bond interface (Baldan, 2012). The peaks and valleys of the surface enhance the bond strength due to the increase in effective area. However, too rough of a surface may result in poor polymer penetrability, void formation, and stress concentration leading to lower bond strength (Prolongo et al., 2006). Deep valleys can lead to trapping of air between the polymer and metal surface. In addition, stress concentration regions can develop at the interface within the polymer around the metal projections, which can lead to weak bonding according to Packham (1992). For the material and conditions considered in this study, best results were obtained when surface roughness was $5.63 \mu\text{m}$.

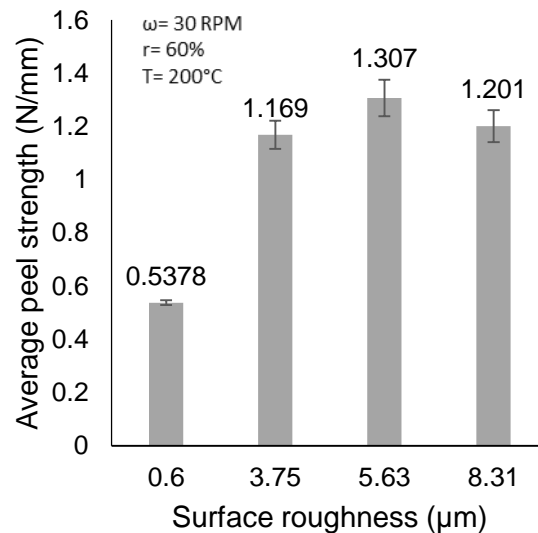


Fig. 13: Peel strength of AL1100-PU-AL1100 fabricated with different surface roughness

values. Data: Mean \pm SD (n=3).

Both cohesive and adhesive failure modes are found in metal/polymer interface bond failure. Cohesive bond failures result in fracture within the polymer core and are characterized by the clear presence of polymer material on matching faces of both adherends. Adhesive failures are characterized by the absence of polymer material on one of the bonding surfaces and failure occurs along the interface between the polymer layer and the adherends (Davis et al., 2010). Observation of the fracture surfaces revealed that adhesive and cohesive failures occurred on all specimens to varying degrees. Analysis of the metal/polymer interfacial fracture surfaces, however, shows notable difference between the bonds created from the roughened surface and those created from the relatively smooth, as-received surface. A general trend was that the higher bond strength specimens showed smaller adhesive failure region and larger cohesive failure region. Comparing Fig. 14 A and Fig. 14 B-D, the failure surfaces for those bonds created with the smooth, as-received surface had more adhesive failure than bonds created with roughened surface. Moreover, increasing the surface roughness caused the transition of failure mode from adhesive to cohesive, which improved the overall adhesion strength (Kim et al., 2010).

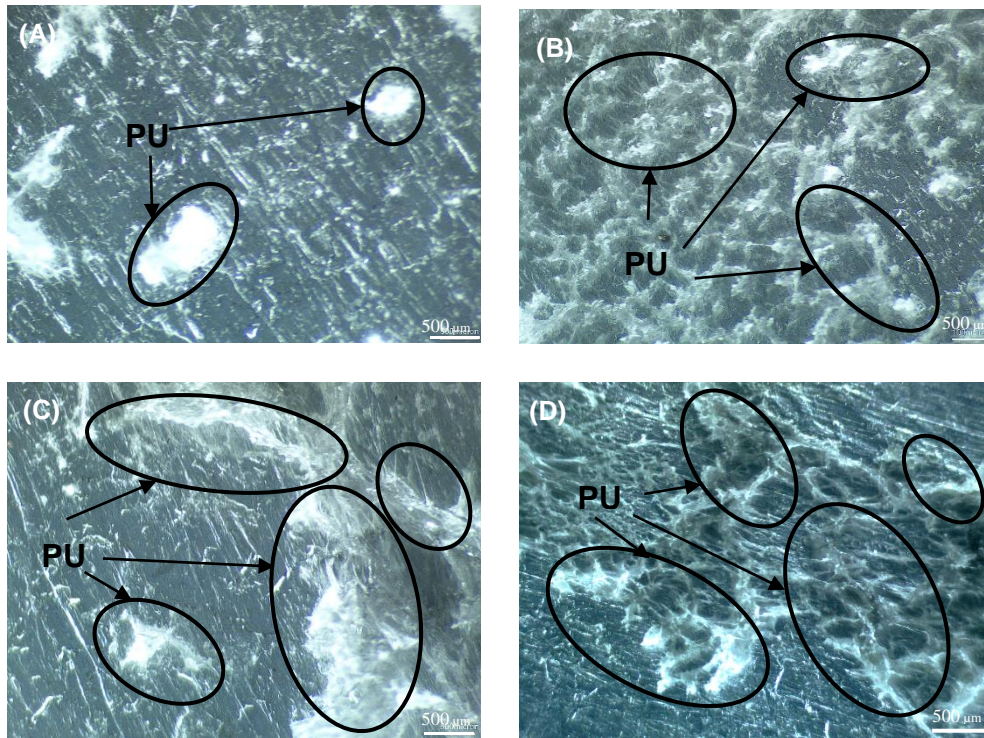


Fig. 14: Fracture surfaces of AL1100/PU after peel test with 60% reduction, 200°C preheating, and 30 rpm rolling speed for different surface roughness values: (A) as-received AL1100 ($R_a=0.6 \mu\text{m}$), (B) sandpaper grit 80 ($R_a=3.75 \mu\text{m}$), (C) sandpaper grit 50 ($R_a=5.63 \mu\text{m}$), and (D) sandpaper grit 36 ($R_a= 8.31 \mu\text{m}$).

3.3.1.2 Effect of preheating temperature on adhesion strength

The relationship between adhesion bond strength and the preheat temperature of AL1100 strips is shown in Fig. 15. The experiments were conducted at the thickness reduction of 60%, surface roughness of $5.63 \mu\text{m}$, and rolling speed of 30 rpm. It was observed that with increasing preheat temperatures the adhesion strength increased to 1.307 N/mm at 200°C and then it dropped down to 1.011 N/mm at 240°C . At 240°C , excessive loss of PU was observed leading to decrease in the bond strength. When bonding experiments were conducted outside the temperature range, at 150°C and 250°C , no successful bonds were created. An increase in the

rolling temperature may lead to a greater degree of recovery and recrystallization of the metals and softening of the materials. As the metals become softer, the effect of plastic deformation increases, resulting in fragmentation of the oxide layer and formation of a stronger bond between the warm rolled materials (Peng et al., 1999). Rolling temperature greatly helped the polyurethane sheet to become soft and to interlock in the AL1100 rough surface.

In general, the temperature directly influences the behavior of a polymer material. The polyurethane sheet used in this study was a medium-hard segment polymer. The softening and melting points determined by visual observation in a melting point capillary were approximately 200°C and 243°C, respectively (Oertel, 1994). When the preheat temperature was 170°C, below the softening point, the polymer flow was restricted, and therefore, it resulted in the final total thickness of 1 mm with rolling operation set to 60% reduction. As the temperature was raised to 200°C and 240°C, the measured final total thicknesses were below the expected value by 15% and 30%, respectively. At higher temperatures, some of the core material melted and squeezed out of the sample.

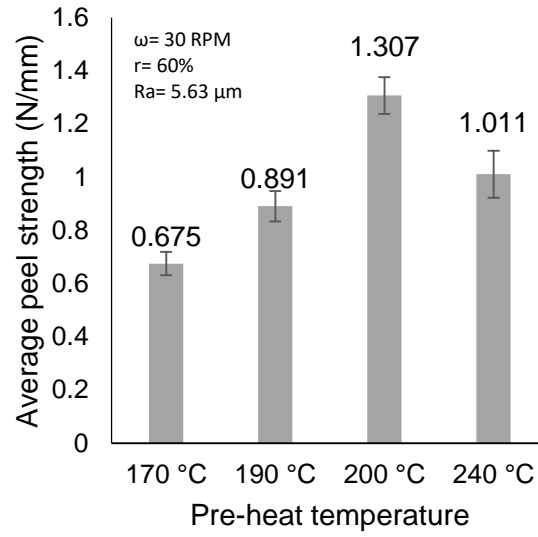


Fig. 15: Variation in peel strength of AL1100-PU-AL1100 versus preheat temperature.

Data: Mean \pm SD (n=3).

3.3.1.3 Effect of rolling speed on adhesion strength

The relationship between the adhesion bond strength and the rolling speed is shown in Fig. 16. The adhesion strength was highest at the rolling speed of 30 rpm. In contrast, the adhesion strength is typically the highest at a lower rolling speed and decreases as the rolling speed is increased for cold roll-bonding. It has been verified by Abbasi and Toroghinejad (2010) that higher rolling speeds lead to shorter bond times to effectively apply pressure on the rolled sheets resulting in a sharp decrease in the adhesion strength. The bond times for this study are calculated and listed in Table 5 for reference. It is observed that as the rolling speed increases, the contact time decreases. In WRB, however, the temperature influences the bonding as described in Fig. 15. In general, higher temperature helps to interlock polymer with the metal surface. At low rolling speeds, the quenching of heated workpiece is significant due to long contact times with the cold rolls resulting in low bond strength. On the other hand, the

temperature is relatively uniform and maintained better at higher rolling speeds. Therefore in WRB, two competing effects, i.e., the bond time and temperature, contribute to the adhesion strength as illustrated in Fig. 17. At 18 rpm, the metal sheets and polymer core are quenched significantly leading to the low bond strength although the contact time is long. On the other extreme high rolling speed, the bond is insufficient for robust adhesion. For the conditions in this study, the optimal rolling speed was at 30 rpm.

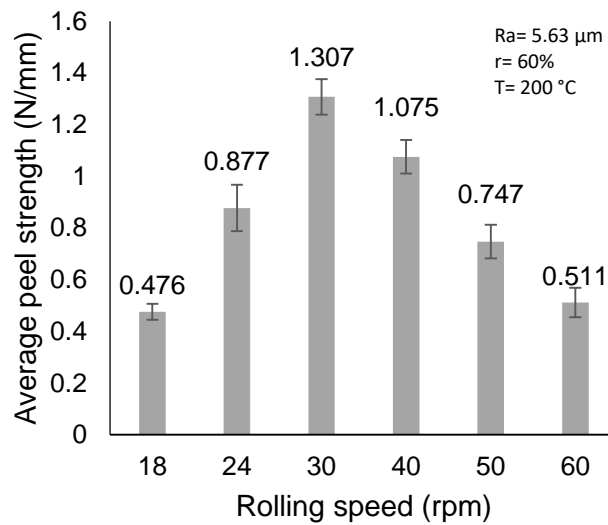


Fig. 16: Variation in peel strength of Al 1100/PU/AL1100 versus rolling speed. Data: Mean \pm SD (n=3).

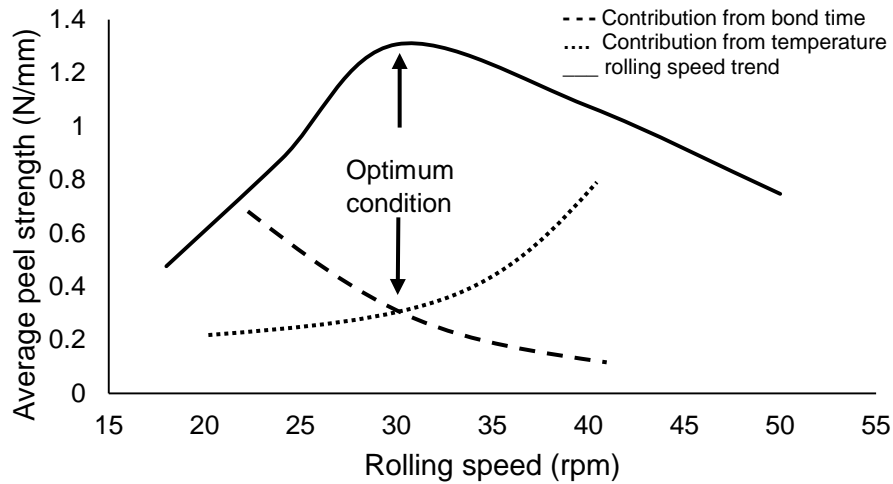


Fig. 17: Schematic diagram of optimum rolling speed.

Table 5: Contact times of different rolling speeds.

Rolling speed (rpm)	Contact time (ms)
18	88.3
24	70.6
30	52.9
40	39.7
50	31.7
60	26.4

A separate Design of Experiment (DOE) study was carried out for the rolling speed and preheat temperature to determine the optimal condition and to understand interaction effects. A fractional factorial design was employed with three levels (low, medium, and high) for the two factors, the temperature and the rolling speed. The settings were selected before, at, and after the peaks of the two factors from previous results and are summarized in the Table 6.

Table 6: The settings and results of design of experiments.

Run number	Temperature (°C)	Rolling speed (rpm)	Peel strength (N/mm)
1	200	30	1.307
2	240	40	0.563
3	240	18	0.349
4	240	30	1.011
5	170	18	0.311
6	170	40	0.844

The resulting plots of DOE are shown in Fig. 18. Fig. 18(A) shows the prediction profiles of the optimal temperature and rolling speed. The optimal values predicted for the preheat temperature and rolling speed that maximized the peel strength were 200.2°C and 29.7 rpm, respectively, which support the findings in previous results. The interaction plots are provided in Fig. 18(B), which shows a slight interaction at low rolling speeds (around 18 rpm). This interaction, however, is not significant as its p-value was 0.28.

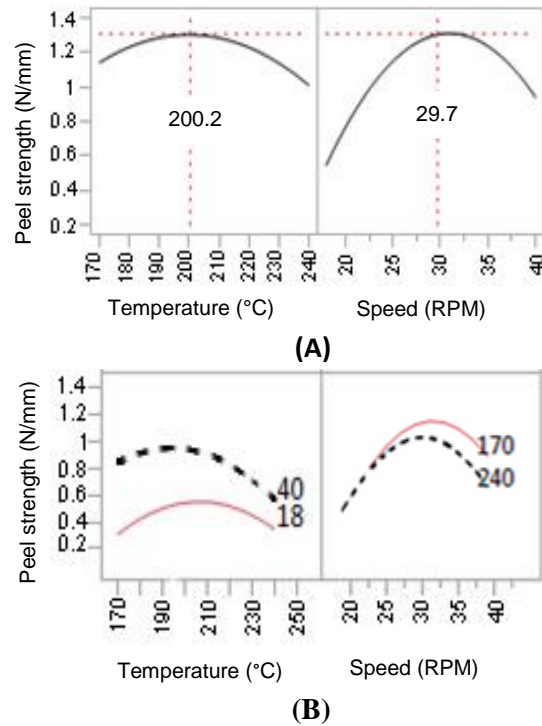


Fig. 18: DOE study results. (A) Prediction profiles of preheat temperature and rolling speed. (B) Interaction plot of preheat temperature and rolling speed parameters.

3.3.1.4 Effect of thickness reduction on adhesion strength

The effect of total reduction in thickness on the bond strength of AL1100-PU-AL1100 sandwich composite is shown in Fig. 19. During simultaneous rolling of AL1100-PU-AL1100 sandwich sheets, the brittle surface layers of AL1100 from sanding are subjected to high normal pressure resulting in the formation of surface cracks in the rolling direction (Soltan Ali Nezhad and Haerian Ardakani, 2009). The PU flows into these cracks and interlocks with the metal surface achieving adhesion between the rolled layers. According to Abbasi and Toroghinejad (2010), the increase in bond strength at higher total thickness reduction is due to the increase of mean contact pressure and more overlapping of exposed surface at the interface. At thickness reductions up to 60%, the soft polymer core tends to take the thickness reduction without any

fracture in the skins or the core material as shown in Fig. 20. At higher total thickness reduction of 75%, some of the PU squeezed out of the sample during rolling due to the high normal pressure that the sample exhibited, but that lead to an increase in the overlapping of the exposed surfaces at the interface. In general, increasing the reduction ratio lead to an increase in the contact area in between the interfaces of the metal-polymer sandwich composites. The optimum thickness reduction was at 60% reduction for the current study.

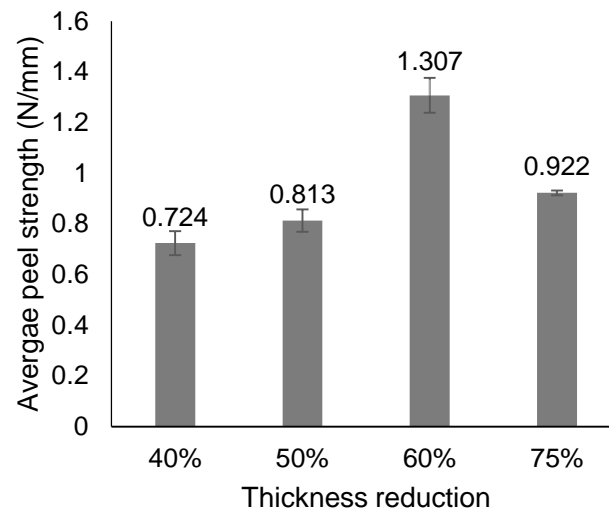


Fig. 19: Variation in peel strength of AL1100-PU-AL1100 versus thickness reduction.

Data: Mean \pm SD (n=3).

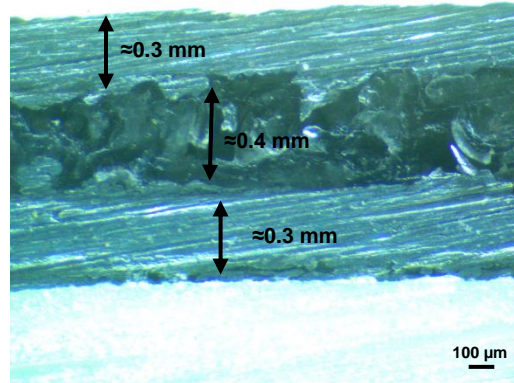


Fig. 20: Cross sectional of AL1100-PU-AL1100 sample with 60% thickness reduction.

3.3.2 Small punch test results

3.3.2.1 Small punch test

The roll bonded AL1100-PU-AL1100 sandwich composite have been analyzed using the SPT at various thickness reductions. The laminate composite, ultimate load, average stiffness, specific load, and specific fracture energy are reported in this section.

A typical load-displacement curve of the AL1100-PU-AL1100 from a SPT is shown in Fig. 21. The curve may be divided into four different stages as follows (Wang et al., 2008):

- I. Elastic bending deformation, which the entire sample undergoes elastic deformation.
- II. Plastic bending deformation where transition from purely elastic behavior to elastic-plastic behavior takes place.
- III. Membrane stretching, which the deformation of the sample is not caused by a bending stress but by a stretching stress around the contact area between the ball and the sample.
- IV. Plastic instability, which corresponding to the propagation of the main crack.

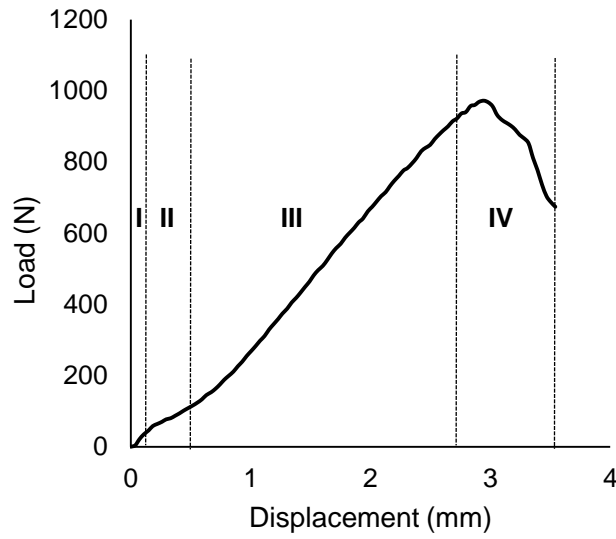


Fig. 21: Typical load displacement curve of AL1100-PU-AL1100 SPT sample.

The ultimate loads at various thickness reductions for AL1100 and AL1100-PU-AL1100 samples are shown in Fig. 22. The ultimate load is taken at the peak load, which indicate the onset of rupture before the complete failure in the load-displacement curve (Tang et al., 2003). As expected, the ultimate load decreased as the specimen became thinner with higher thickness reductions for both AL1100 and AL1100-PU-AL1100 sandwich composite samples. The AL1100 monolayer samples were higher in the ultimate loads except for the largest thickness reduction at 75%. The presence of a soft, thin layer at the center of laminated structure helps to arrest cracks propagating through the whole structure during the SPT. In various other laminate systems that have alternating soft and hard layers, layer delamination may occur ahead of an advancing crack, and the crack may be deflected or blunted (Lesuer et al., 1996). Therefore, further crack growth requires re-nucleation of the void in the hard layer (Suresh, 1983). This arresting and re-nucleation process results in a significant increase in the amount of energy required for the crack to grow during the SPT (Ohashi et al., 1992).

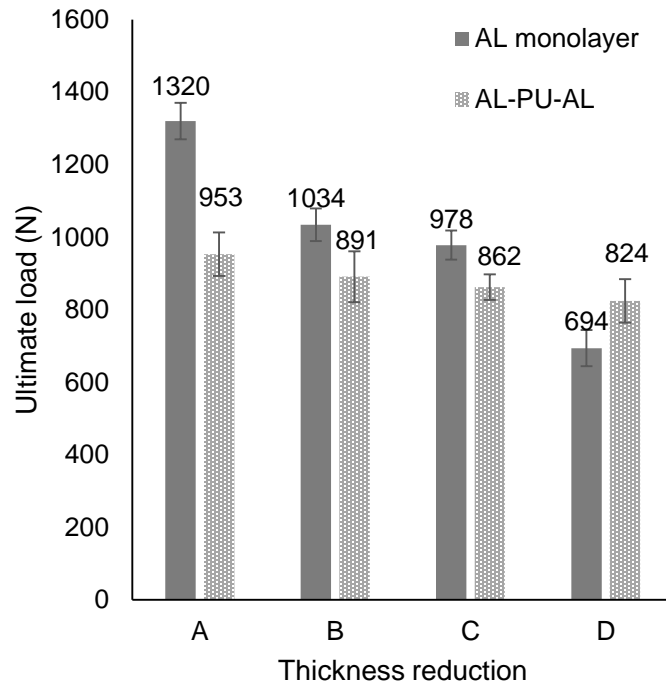


Fig. 22: Ultimate load versus different thickness reductions. Data: Average (n=3).

Fig. 23 shows the specific load calculated from the ultimate load for all AL1100 and AL1100-PU-AL1100 samples. As expected, the AL1100 samples almost have the same specific load ratio regardless of the sample thickness used for testing. On the other hand, the AL1100-PU-AL1100 sandwich composites samples showed significant increase in the specific load at thickness reduction of 50% or more.

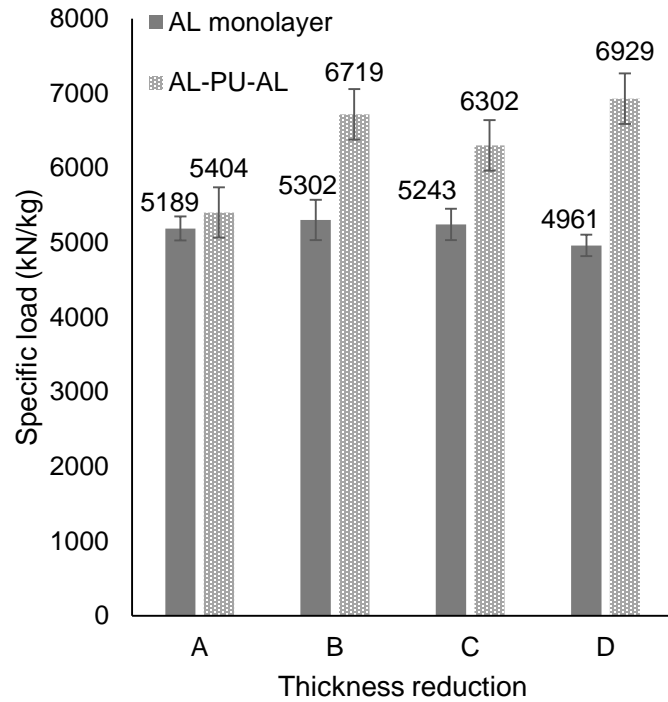


Fig. 23: Specific load for different thickness reductions. Data: average (n=3).

The average stiffness may be measured by calculating the slope of stage I from the load-displacement curve, and the values are summarized in Fig. 24. It is clearly showed that the AL1100 monolayer samples are stiffer than the AL1100-PU-AL1100 samples, since the composites include softer PU layer that reduces the elastic modulus.

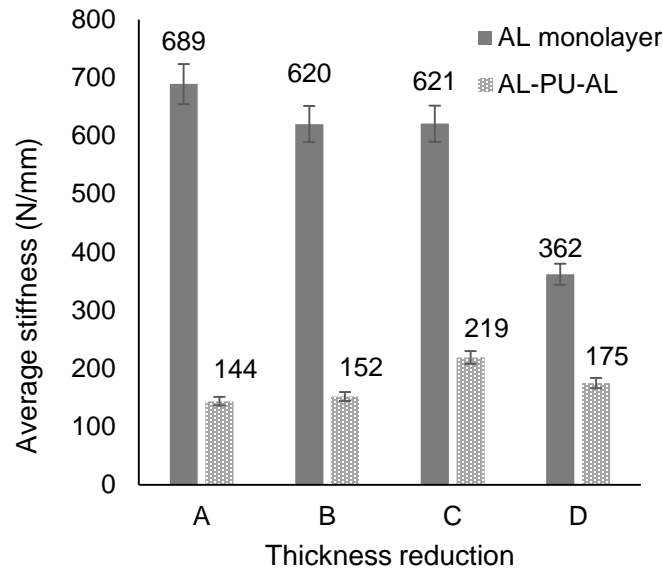


Fig. 24: Average stiffness for different thickness reductions. Data: Average (n=3).

The specific fracture energy of the SPT is calculated by adding the area under the load-displacement curve until 20% load drop is reached after the ultimate load, which is defined as the failure by European standard (CWA) (Standard, 2007a), and dividing the total area by the sample weight. The specific fracture energy is a measure of material's ability to absorb energy before breaking (Mak, 2011). Fig. 25 shows the specific fracture energy results for various thickness reductions for AL1100 and AL1100-PU-AL1100 sandwich composites. The results of AL1100 samples with various thickness reductions were in the same range except for a slight decrease noted at the highest reduction. At the thickness reductions of 60% and 75%, the sandwich composites had higher specific fracture energy than AL1100 monolayer samples. The sandwich composites at high reductions of 60%, and 75%, absorbed more energy before fracturing, and that might be related to the presence of the thin soft layer that help to arrest cracks from going through the laminate structure.

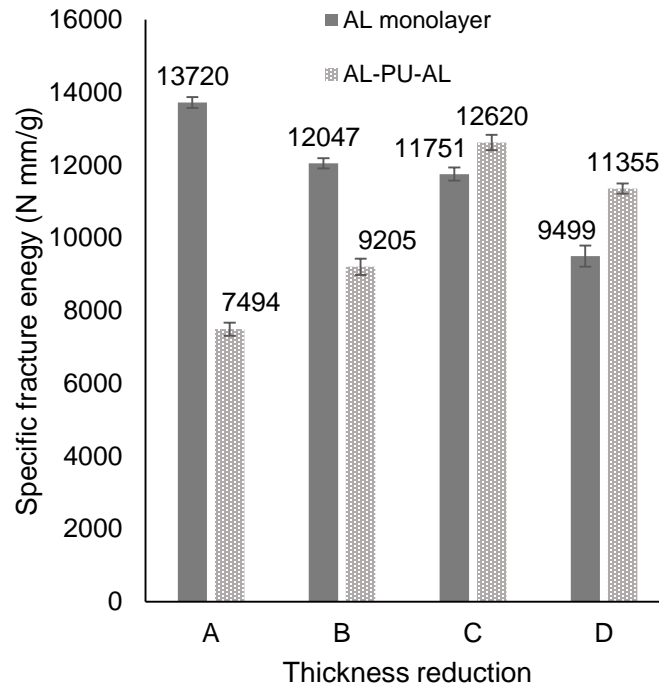


Fig. 25: Specific fracture energy for SPT with various thickness reductions. Data: Average (n=3).

3.3.2.2 Fracture analysis

A detailed fracture analysis was carried out for the AL1100-PU-AL1100 sandwich composite and the monolayers samples at various thickness ratios. Fig. 26 shows the cross sectional images of the AL1100-PU-AL1100 sandwich composite and AL1100 monolayer samples after fracture. The AL1100 samples showed complete fracture through the thickness without any crack arresting or blunting. The crack propagated from the outer layer to the inner layer in a straight path. On the other hand, the samples of AL1100-PU-AL1100 with reductions at 40% and 50% were severely damaged at both skin layers with delamination at the interface. Since the bonding at the interface was not strong enough to hold the structure during the SPT, each skin was individually bearing the load. The samples with reductions at 60% and 75% were

only fractured at the outer skin. Clearly, these soft interfaces of AL1100-PU-AL1100 samples in Fig. 26 indicate arresting the crack regions, in which the subsequent crack growth required re-nucleation, and that results in significant amount of energy needed to crack growth during the SPT.

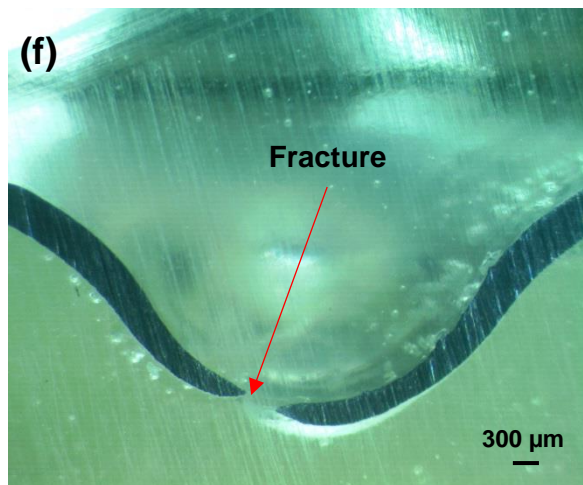
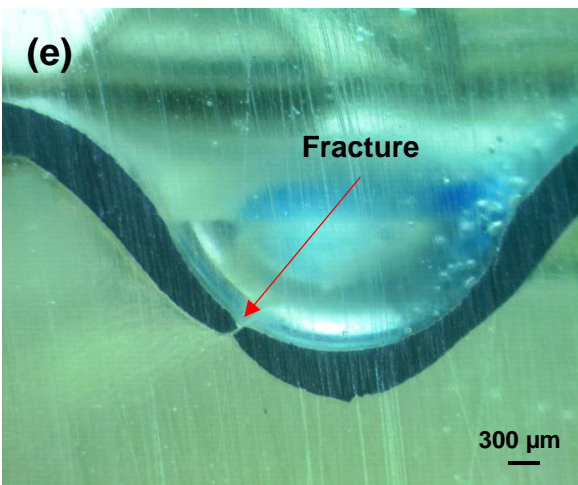
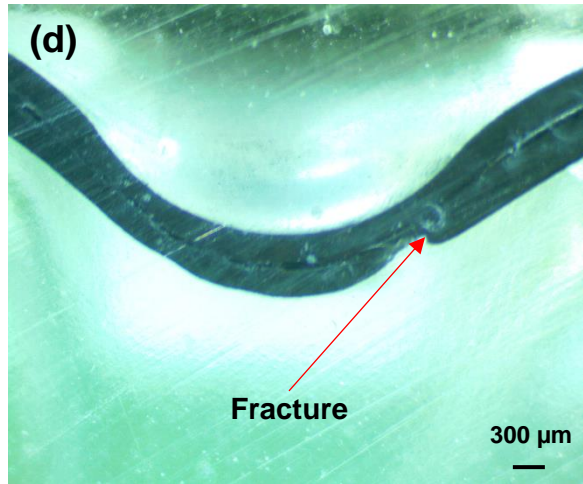
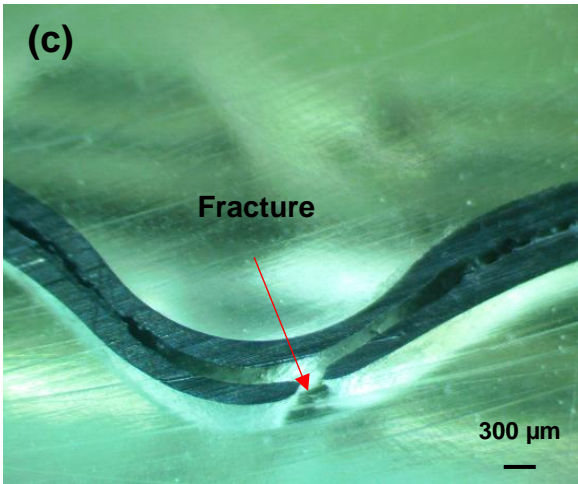
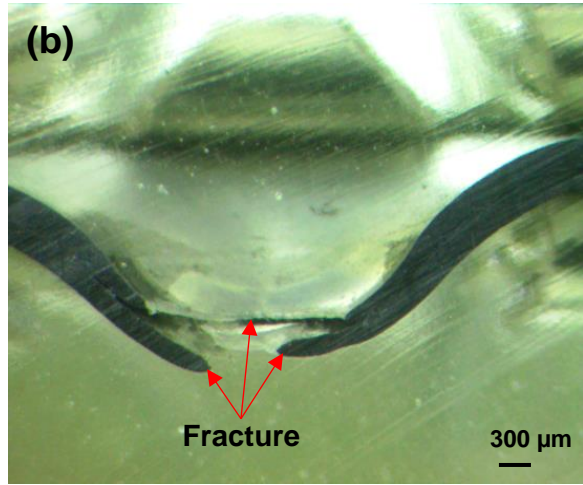
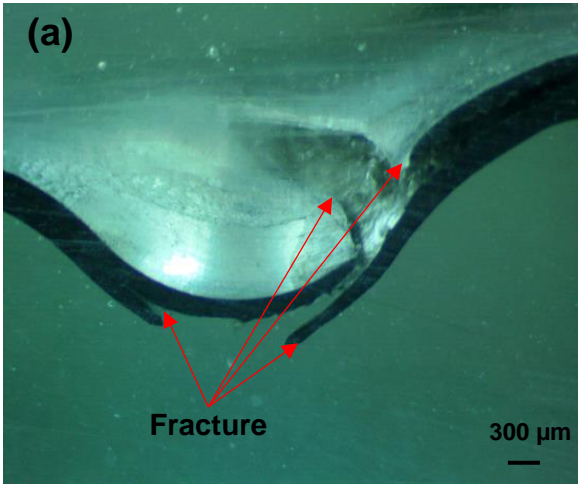


Fig. 26: Cross sectional images of fractured samples of SPT for different thickness reductions: (a) 40% (AL-PU-AL), (b) 50% (AL-PU-AL), (c) 60% (AL-PU-AL), (d) 75% (AL-PU-AL), (e) 50% (AL monolayer), and (f) 75% (AL monolayer).

A detailed analysis was carried out for the AL1100-PU-AL1100 sandwich composites at thickness reduction ratio of 75%. The load-displacement curves of the AL1100 and AL1100-PU-AL1100 sandwich composite samples are compared in Fig. 27. In the first and second stages, AL1100 samples stiffer than the sandwich composites, because AL1100 monolayer samples high elastic modulus as described on the average stiffness results. In the third stage, the sandwich composites showed more fracture resistance compared to the AL1100 monolayer samples, and that can be noticed from the behavior of the curve at stage III for both samples. At the peak portion of both curves, the sandwich composites samples exhibited prolonged fracture, which indicated good crack arresting between the laminates structure before complete failure. The fracture energy absorbed within 5% of the peak load for the composite and monolayer samples were $480 \pm 26 \text{ N}\cdot\text{mm}$ and $349 \pm 19 \text{ N}\cdot\text{mm}$, respectively from the three repeated tests. The difference in fracture behavior between the sandwich composites and the bulk materials as shown in Fig. 26 (d) and (f) resulted in differences in the toughness, the sample with laminates structure showed an increased toughness as shown in Fig. 27, and same behavior was verified by (Lesuer et al., 1996).

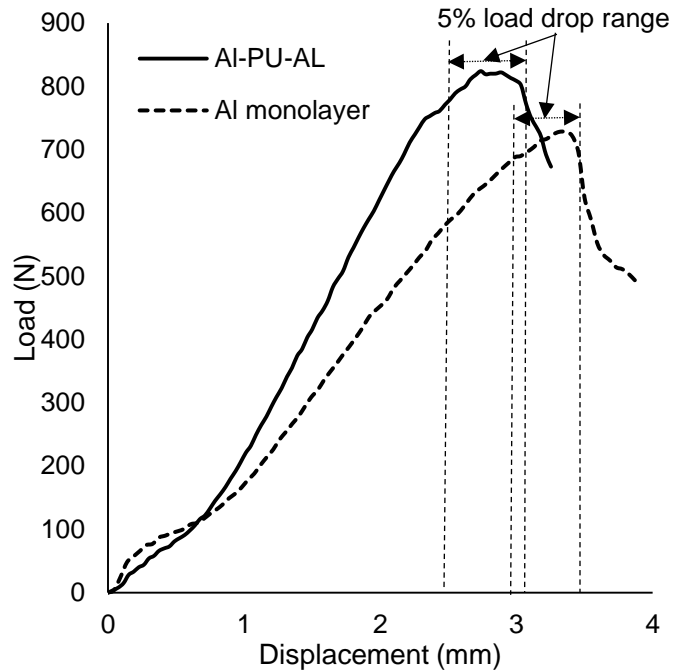


Fig. 27: Load versus displacement curves for AL1100-PU-AL1100 sandwich composites and AL1100 samples for thickness reduction of 75%.

Micrographs of cross sections at four different loads and stages (200 N, 500 N, 700 N, and 800 N) were taken to analyze the thinning of the upper and lower skins of the composite samples as shown in Fig. 28. Table 7 summarizes the measured dimensions of the upper and lower skins. At 200 N, which is in the beginning of stage III (stretching stage), there is no noticeable difference in thickness; however, the two samples considered to be in the beginning of the stretching stage. At 500 N, which is in the end of stage III, there is a difference in the thickness dimension; the lower skin is thinner than the upper skin. At this point, the sample is at the end of the stretching stage, and at this stage the lower skin is under severe stretching stress (Cheon and Kim, 1996). At 700 N, which is at the beginning of stage IV, the thinning effect was clear and observed at the lower skin, and this directly affected the peak load. At 800 N, which is at the end of stage IV, it is clearly noticed the fracture happened at the lower skin.

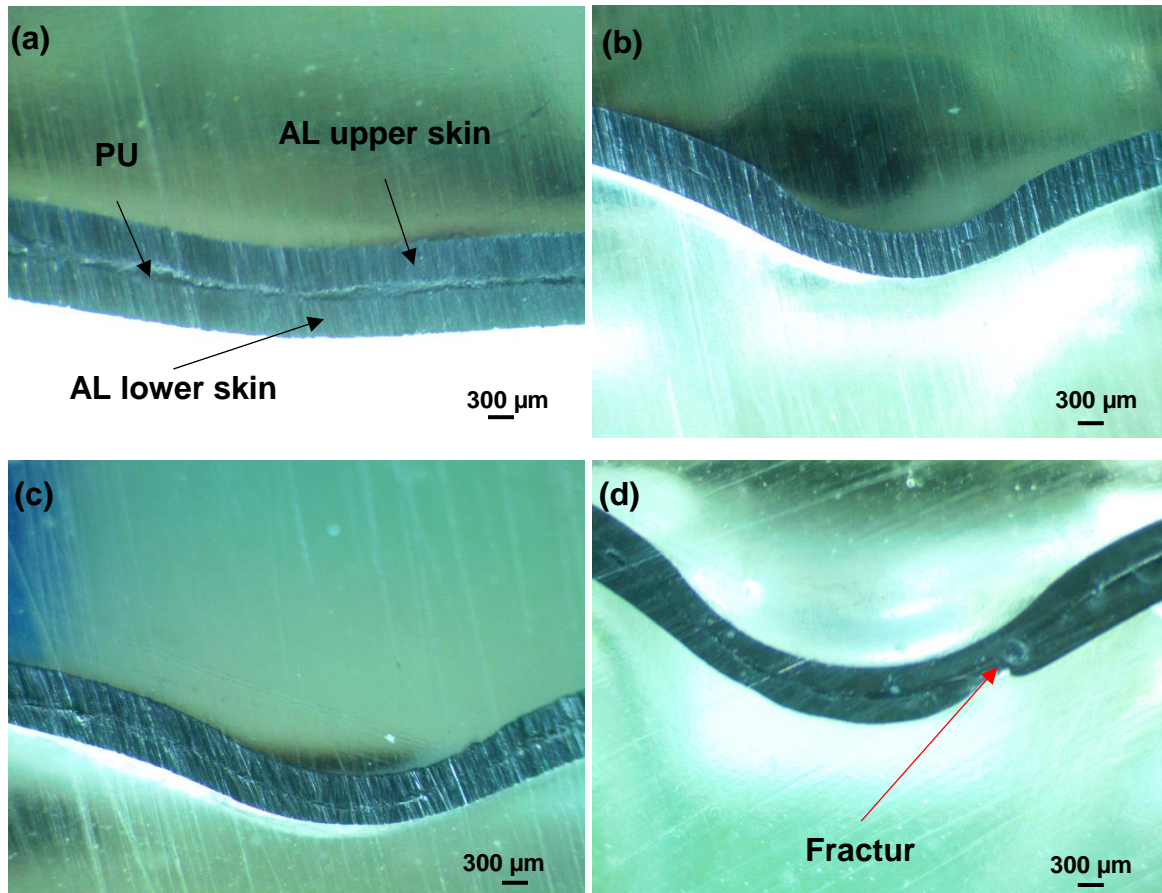


Fig. 28: Cross sectional images for the 75% thickness reduction of AL1100-PU-AL1100 sandwich composites at different SPT loads: (a) 200 N, (b) 500 N, (c) 700 N, and (d) 800 N.

Table 7: Thickness measurements at different SPT loads.

Load (N)	Upper skin (μm)	Lower skin (μm)
200	326	320
500	295	281
700	290	180
800	280	160

3.4 Conclusions

In this chapter, AL1100-PU-AL1100 sandwich composite was fabricated by WRB process to achieve a direct bonding of layers without a glue agent. The effects of processing parameters including the surface roughness, preheat temperature, rolling speed, and total thickness reduction on peel strength and mechanical properties were investigated. The conclusions drawn from this study can be summarized as follows:

- Experimental results indicated that the mechanical interlocking was the primary adhesion mechanism for AL1100 and PU in WRB process. As surface roughness increases, the effective contact area increases, but chances for poor polymer penetration and stress concentration may increase. For the material and conditions considered, an optimal surface roughness was observed at 5.63 μm .
- The failure mode of warm roll bonded AL1100/PU laminate composite changed from adhesive to cohesive as the surface roughness increased.
- The bond strength increased with higher thickness reduction because of the increase in the mean contact pressure and more overlapping of exposed surface at the interface, but excessive reduction at 75% led to inferior bonds due to the onset of mechanical instability.
- The presence of a polymer layer in a metal-polymer-metal sandwich composite helps to increase the specific load with respect to other AL1100 samples by 26%, 20%, and 36% at reduction ratios of 50%, 60%, and 75%, respectively.

- At high reduction ratios of 60%, and 75%, the specific fracture energy of the sandwich composites samples improved by 10%, and 20%, respectively, with respect to the AL1100 samples.
- The fracture analysis results showed that the presence of a soft, thin layer at the center of laminated structure helps to arrest cracks propagating through the whole structure during the SPT.

CHAPTER 4 ROLL-BONDING OF GLASS FIBER REINFORCED METAL-POLYMER-METAL SANDWICH COMPOSITES

4.1 Introduction

Metal-polymer-metal sandwich composites are considered an innovative substitute to the commercial steel sheets in the automotive industry due to weight-saving potential and enhanced damping properties (Harhash et al., 2017). Roll bonding has been used to manufacture metal-polymer-metal sandwich composites due to its simplicity and cost-effective production (Carradò et al., 2010). The sandwich composite consists of steel skins and polypropylene (PP) core roll bonded using an indirect adhesion (glue between layers) confirmed good formability (Carradò et al., 2011a). Mousa and Kim (2015b) introduced the direct adhesion (without glue) roll bonding technique to produce an aluminum 1100 (AL1100) and polyurethane (PU) sandwich composite. Moreover, Mousa and Kim (2017) found that the presence of the soft PU layer in the AL1100-PU-AL1100 sandwich composite helps to increase the specific fracture energy compared with the AL1100 monolayer.

Despite the simplicity of direct and indirect roll bonding of metal-polymer sandwich composites, they have not gained widespread usage in the automobile industry because of their lack in adhesion and shear performances (Sokolova et al., 2010). Various approaches have been investigated to enhance the adhesion and the shear strengths of the roll-bonded metal-polymer-metal sandwich composites. Carradò et al. (2011b) used various surface treatments (corona discharge and plasma treatment) on the metal surface to increase the wettability and found that the adhesion strength and the formability of the indirect roll bonded composites increased when compared to the untreated samples. Sokolova et al. (2011) used embedded solid and mesh steel inlays between the steel-polymer sandwich composite layers to improve the adhesion

performance, and a slight improvement was achieved while formability improved by 9% due to the mesh inlays. Mousa and Kim (2015a) used roughened metal surface by sandpaper to assure good mechanical interlocking between the layers of the samples; this led to an enhancement in the adhesion strength.

In this study, a new technique is introduced to fabricate fiber-reinforced, roll-bonded metal-polymer sandwich composites for enhanced adhesion and shear performance. In general, fiber-reinforced composites help to increase various properties including, strength (Dymáček, 2001), stiffness (Mallick, 2007), impact resistance (Abdulmajeed et al., 2011), and damage tolerance (Reyes and Kang, 2007). In this work, glass fibers were introduced at the interface between the metal skins and the polymer core using the warm roll bonding (WRB) process. The effects of reinforcing glass fibers on the mechanical and bonding properties were investigated by performing T-peel test, single lap shear test, and small punch test (SPT) as well as by electron microscopy analysis.

4.2 Experimental procedure

The sandwich composites consist of two strips of commercially pure aluminum (AL1100) for the skin with initial dimension of 70 mm × 20 mm × 0.5 mm, and a polyurethane (PU) sheet at the core with initial dimension of 60 mm × 20 mm × 0.8 mm. S-glass fibers were used as the reinforcing material. S-glass fibers have high strength (4.75 GPa) and their operating temperature is wide, -269°C to 650°C (Mukhopadhyay, 2005). These properties are crucial for a successful roll bonding process, which enables the reinforcement phases to survive the high pressure involved with bonding at elevated temperatures. Since s-glass fibers were received as bundles, following steps were performed to separate them. First, ball milling with a plastic ball

of 9 mm diameter was used for 30 seconds to separate the large bundles in an 8000M milling machine. Then the glass fibers were sonicated in an ethanol solution for two hours after which they were left for 24 hours to dry. Fig. 29 shows the glass fibers bundles before and after ball milling. The original glass fibers had a diameter about $\text{Ø}22 \mu\text{m}$ and a length of 3.4 mm. The average diameter and length of a random sample from the milled and dried glass fibers were $\text{Ø}21 \pm 1.1 \mu\text{m}$ and $2.8 \pm 0.47 \text{ mm}$ ($n=20$), respectively. The specifications of AL1100 strips, PU sheets, and s-glass fibers are summarized in Table 8.

Table 8: Specification of AL1100 strip, PU sheet, and glass fiber.

Material	Chemical composition (wt.%)	Tensile Strength (MPa)	Yield Strength (MPa)	Elongation (%)
AL1100	99.61 Al, 0.11 Si, 0.55 Fe, 0.11 Cu, and 0.07 others	85	33	30
S-Glass (Nadkarni and Ayodhya, 1993)	65 SiO ₂ , 25 Al ₂ O ₃ , 10 MgO	4750	206	5.7
Material	Shore Durometer (ASTM D2240-64T)	Compression Set (ASTM D395-61, Method B) 22 Hrs. @ 158 F	Ultimate Tensile Strength (ASTM D412-61T)	
PU	60 A (medium hard)	30% Max	21 MPa	

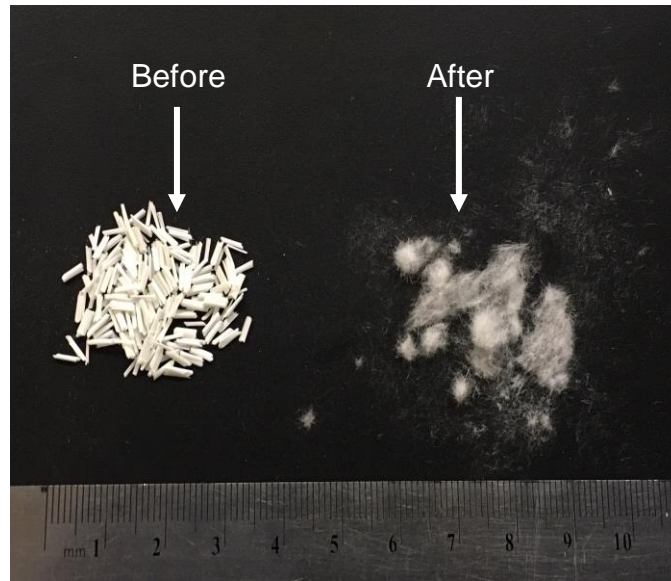


Fig. 29: S-glass fibers before and after ball milling for 30 seconds.

The procedure for specimen preparation is illustrated in Fig. 30. It is critical to clean the surface and remove any contamination before rolling to produce a satisfactory bond in WRB. The procedure used for all sample preparation was to first degrease the surface in ethanol, followed by sanding the surface with 50-grit sandpaper to generate a fresh surface to facilitate the bonding. Then, the glass fibers were applied on the metal skins as shown in Fig. 30. The ball milled fibers were stirred in a blender with a blunt blade for 10 sec while the aluminum skins were hanged horizontally inside the blender to achieve uniform distribution of fibers on the surface of the skin. After assembling the composite as shown in Fig. 30, it was preheated to 200°C and held at that temperature for 3 min before rolling. Rolling speed was set at 30 rpm, which is the optimum rolling speed needed to produce a robust bond between the sandwich layers according to our previous study (Mousa and Kim, 2015b). Two different thickness reductions, 60% and 75%, were used in the experiments. The reinforced sandwich composites

were weighed before and after applying the glass fibers, which account for about 0.25-0.30% of the total weight.

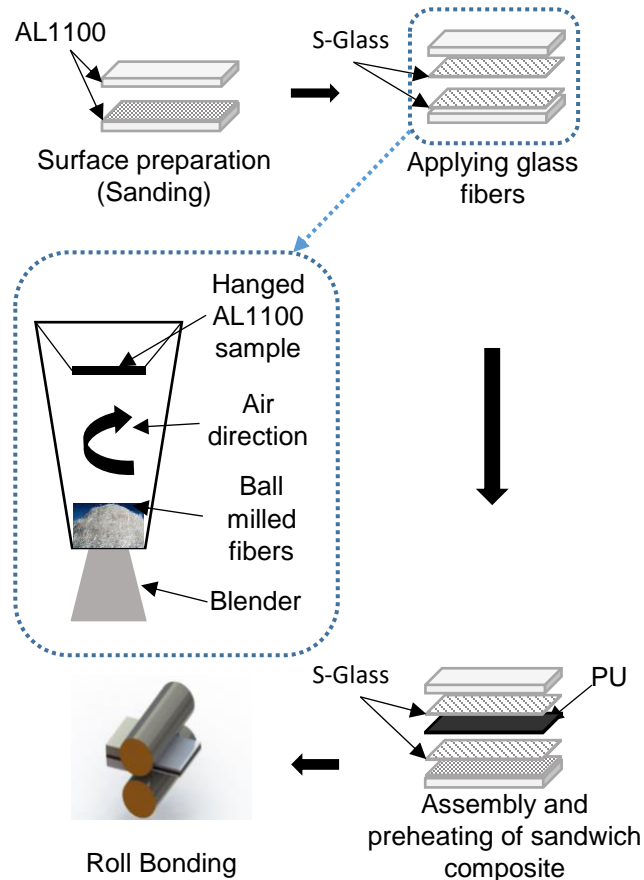


Fig. 30: A schematic illustration of fabricating fiber-reinforced, roll-bonding of metal-polymer composites.

The adhesion between the core and the metal sheets was investigated by a T (180°) peel test according to the DIN53282 as illustrated as described in Chapter 3. The peel test was performed using a universal testing machine (TestResources Inc.) with a crosshead speed of 20 mm/min.

The tensile lap-shear strength between the metal skins and the polymer core was measured by a standard lap-shear test, following ASTM D 1002-01. The 70 mm × 20 mm × 0.88

mm metal-polymer sandwich composite samples have opposing notches with a displacement of 10 mm as shown in Fig. 31(a). The shear area was 200 mm² and the cutting clearance was 1 mm.

The shear strength (τ) is defined as following:

$$\tau = \frac{F_{\max} (N)}{A (mm^2)} \quad (2)$$

where F_{\max} is the maximum crack force by shear test as noted in the load-displacement curve in Fig. 31(b), and A is the shear area of specimen between the notches. The experiments were repeated three times, and the results were averaged over the three samples.

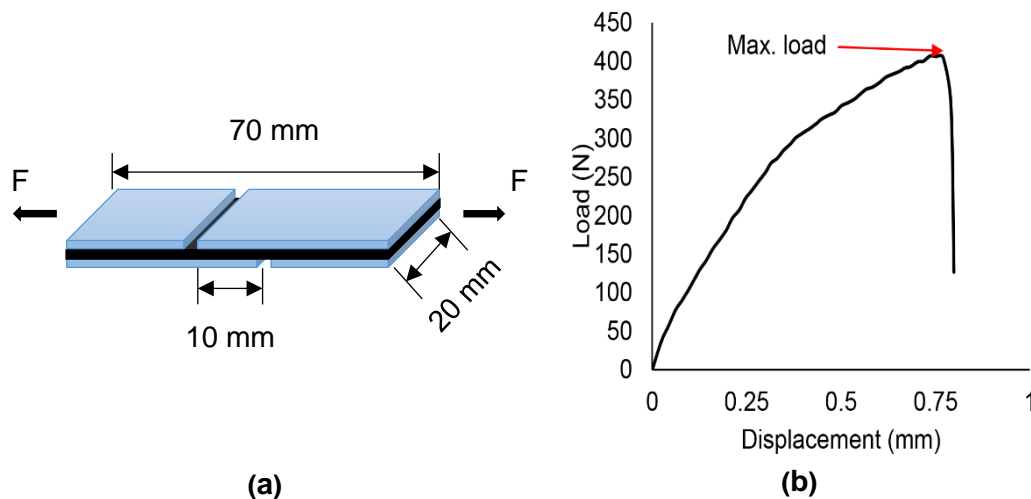


Fig. 31: (a) Sample geometry of the shear test, and (b) The load versus displacement of a shear test.

The small punch test (SPT) was carried out using an experimental device as shown in Chapter 3. The experimental setup included a disc specimen, a 6 mm diameter ceramic ball, and a specimen holder that consisted of an upper and lower die on which the sample was placed and centered on a 10 mm hole. The sample was set between the upper and lower dies, which was

tightened with clamping screws. The SPT were conducted at a crosshead speed of 0.2 mm/min with load cell of 5 kN capacity. The load and cross head displacement were recorded simultaneously over time.

To better understand the toughening mechanisms involved, the fracture surface was coated and analyzed by a Philip XL30 scanning electron microscope (SEM) at voltage acceleration of 10 kV.

4.3 Results and discussion

The reinforcing effects of glass fibers on the adhesion and shear resistance of metal-polymer sandwich composites were investigated. The T-peel test, single lap shear test, and small punch test were used to evaluate the mechanical and bonding properties of these composites.

4.3.1 T-peel test and single lap shear test

The T-peel test has been used extensively to evaluate the bonding strength of laminated composites. Generally, Mode I fracture is associated with peeling when a load is applied perpendicular to the surface of the interface. During Mode I failure, the crack propagates in a stable manner (Rolfe and Barsom, 1977). The effect of the reinforcement of glass fiber on the peel strength of roll bonded sandwich composites at various reductions is shown in Fig. 32. The results show that the presence of glass fibers at the interface has little impact on the peel strength. The average peel strength from repeated testing shows 8% and 7% increase for thickness reductions of 60% and 75%, respectively although the values are within the range of experimental variation.

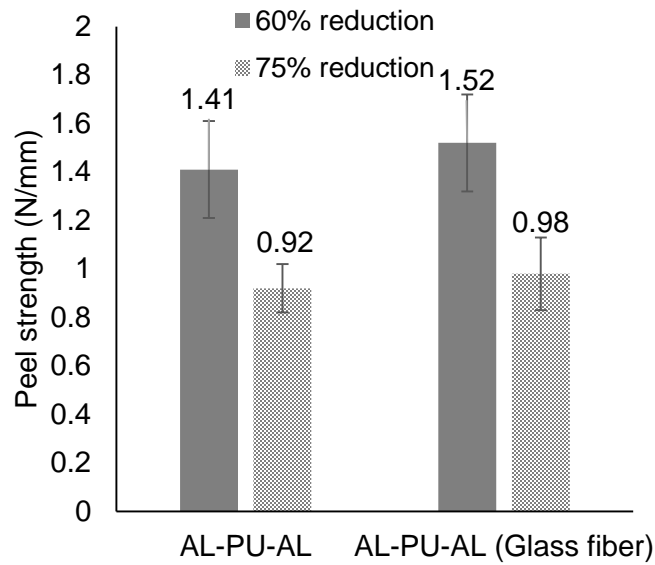


Fig. 32: Peel strength measurements of the samples with and without reinforcement at reductions thickness of 60% and 75%. Mean \pm SD (n=3).

Single lap shear testing is a method for testing the shear strength of laminated composites by pulling bonded layers along the plane of adhesion. The Mode II failure is associated with shear test since the shear occurs in the plane of the interface (Mower and Li, 1987). The experimental results obtained by shear testing for the reinforced and unreinforced sandwich composites for different thickness reductions of 60% and 75% are shown in Fig. 33. The shear resistance of the glass fiber reinforced sample increased by 39% and 45% for the thickness reductions of 60% and 75%, respectively when compared with the unreinforced sample. Despite the two different reductions, interfacial toughening from the short glass fibers is clearly beneficial. The presence of the glass fibers at the interfaces of the laminated composites helps to delay the occurrence of interfacial slippage and the debonding, which gives higher resistance before failure occurs, thus improving the shear strength (Kim and Mai, 1991).

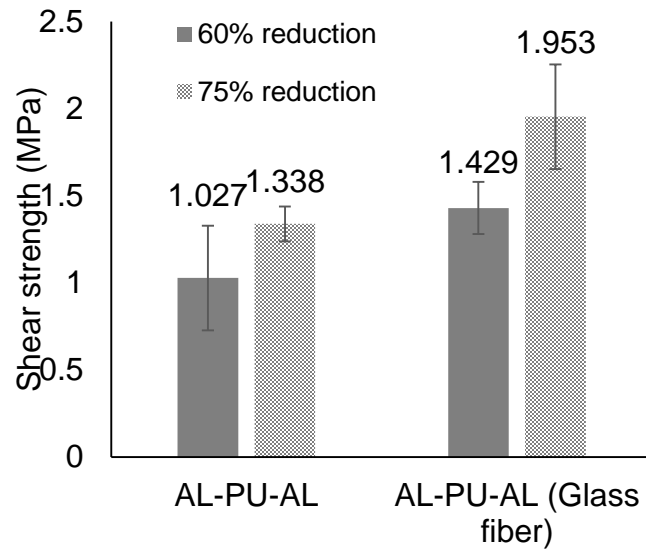


Fig. 33: Shear strength measurements of the samples with and without reinforcement at reduction thicknesses of 60% and 75%. Mean \pm SD (n=3).

4.3.2 Small punch test

The ultimate loads at thickness reductions of 60% and 75% for different samples (AL1100, AL1100-PU-AL1100, and AL1100-PU-AL1100 with reinforcement) are shown in Fig. 34. The ultimate load is taken at the peak load, which indicates the onset of rupture before complete failure occurs (Tang et al., 2003). Despite the various reductions, the presence of the glass fiber helps to increase the ultimate load before complete fracture. The presence of glass fibers at the interface of the laminated soft material and the hard skin material helps to arrest and blunt the cracks from going through the whole structure. In many laminate systems, layer delamination can occur ahead of an advancing crack or as the result of a crack encountering an interface. These local delamination sites can result in crack deflection, which significantly reduces the Mode II component of the local stress intensity because of the large deviations in crack path that are possible. These crack path deviations cause cracks to move away from the

plane experiencing the maximum stress (Lesuer et al., 1996). Therefore, the arresting and re-nucleation process results in a significant increase in the amount of energy required for the cracks to grow during the SPT.

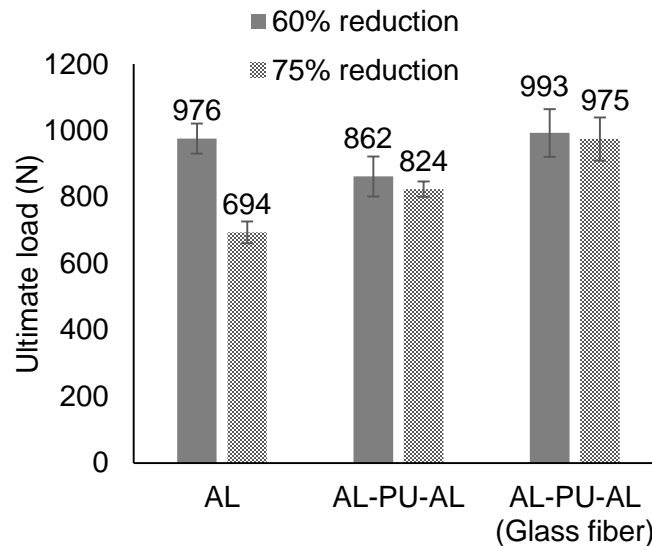


Fig. 34: Ultimate load measurements at reduction thicknesses of 60% and 75% of the samples of AL monolayer, samples of sandwich composites with and without reinforcement. Mean \pm SD (n=3).

The specific load, which is the ratio of the ultimate load to the weight of the sample, was calculated for each sample. Fig. 35 shows the specific load calculated from the ultimate load for all samples at two different thickness reductions of 60% and 75%. As expected, the AL1100 samples have almost the same specific load regardless of the sample thickness used for testing (Mousa and Kim, 2017). On the other hand, the reinforced samples showed a significant increase in the specific load when compared with the bulk AL1100 sample.

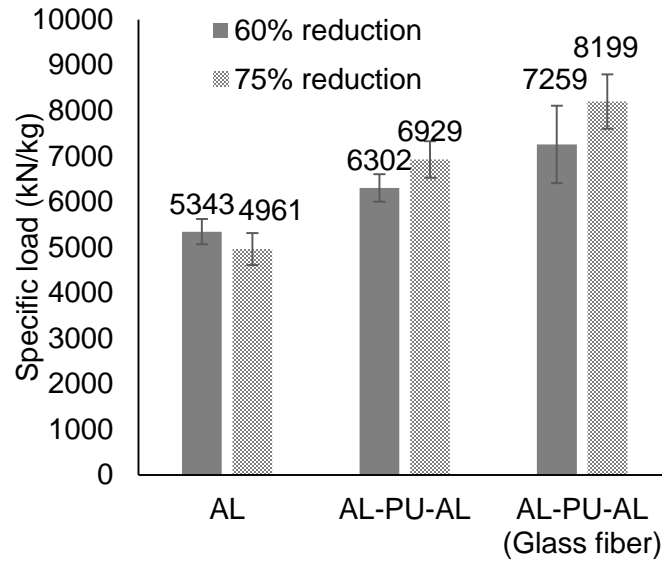


Fig. 35: Specific load measurements at reduction thicknesses of 60% and 75% of the samples of AL monolayer, samples of sandwich composites with and without reinforcement. Mean \pm SD (n=3).

The specific fracture energy of the SPT is calculated by dividing the total area under the load-displacement curve by the sample weight. The total area is calculated until a 20% load drop is reached after the ultimate load, which is the definition of failure by the European standard (CWA) (Standard, 2007b). The specific fracture energy is the measure of material's ability to absorb energy before breaking (Mak, 2011). Fig. 36 shows the specific fracture energy results for AL1100 and AL1100-PU-AL1100 sandwich composites with and without reinforcements at thickness reductions of 60% and 75%. The sandwich composites with glass fiber reinforcement had higher specific fracture energy than AL1100 monolayer and unreinforced sandwich composites samples. The reinforced sandwich composites absorbed more energy before fracturing since the reinforced soft layer at the interface helped to arrest cracks from going through the laminate structure.

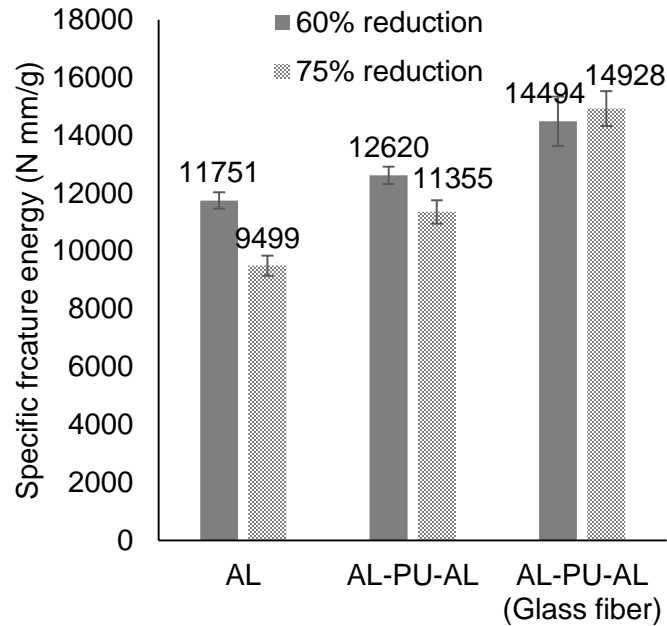


Fig. 36: Specific fracture energy measurements at reduction thicknesses of 60% and 75% of the samples of AL monolayer, samples of sandwich composites with and without reinforcement. Mean \pm SD (n=3).

4.3.3 Observation of failure pattern

A variety of toughening mechanisms (e.g., fiber bridging, debonding, peeling and fracturing) can develop as load is increased at the interface of fiber and resin (Yue and Cheung, 1992). As described by Harris (2013), the fibers are secured by polymer resin prior to failure at the interface of the metal and polymer. As the load is increased during the testing, the crack propagation is obstructed by these fibers. The resistance to shearing at the fiber/matrix interface is derived from the mechanical interlocking between the fiber and resin (Harris, 1978). Further increase of the shear load results in debonding of the fiber from the polymer and can lead to fracture of the fibers. The broken ends of fibers can still add to the frictional work needed in crack propagation. It is clear from Fig. 37 that the toughening mechanisms, such as fiber

bridging, debonding, peeling, and fracturing, are present in the interfacial cracking area. The peel-off marks seen in Fig. 37(a) and (c) show the presence of extensive fiber bridging. Fig. 37(b) and (c) show the details of shear lips and protruding glass fibers, which imply the bridging and pullout mechanisms, leading to an increased shear strength of the reinforced sandwich composites. Some free ends of the fibers as shown in Fig. 37(d) can go deep into the polymer layer, which helps to increase the interfacial strength by increasing the work needed to pullout such fibers.

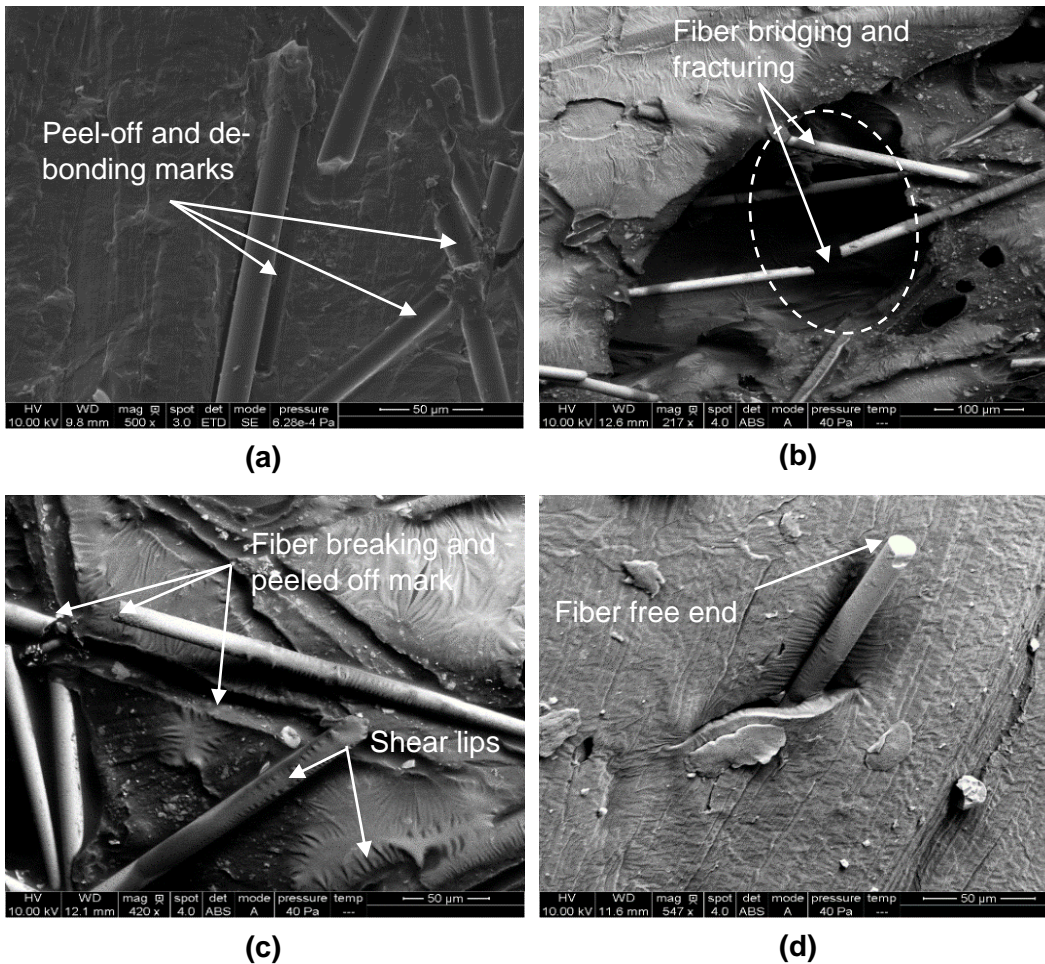


Fig. 37: SEM images of shear failure surfaces with glass-fiber reinforcement: (a) peeled-off and debonding marks of glass fiber (secondary electron detector), (b) fiber bridging and fracture observation (back scattered electron detector), (c) fiber breaking and peeled off marks (back scattered electron detector), and (d) fiber free end (back scattered electron detector).

4.4 Conclusions

Metal-polymer-metal sandwich composites reinforced with glass fibers have been fabricated using the roll bonding process. Observations from the T-peel test, single lap shear

test, and small punch test (SPT) samples suggest that introduced fibers at the interface of roll-bonded metal-polymer sandwich composite influenced tensile and shear failures at the interface. The shear strength of the reinforced composites at thickness reductions of 60% and 75% increased by 39% and 45%, respectively, when compared with the unreinforced composites. The mechanical properties of the reinforced composite measured by the SPT showed improvement in the ultimate load, specific load, and specific fracture energy by 18%, 19%, and 30%, respectively, when compared with the unreinforced composites at thickness reduction of 75%. The presence of different toughening mechanisms introduced by adding glass fibers, including fiber bridging, fiber pull-out, and fiber fracturing were observed in the SEM analysis and contributed to the increase of shear strength at the interface, specific load, and specific fracture energy. The study showed a promising potential of using roll bonding process to mass produce metal-polymer-metal composites with fiber reinforcement at the interface.

CHAPTER 5 SUMMARY AND SCIENTIFIC CONTRIBUTIONS

In this section, the conclusions and contributions of the work carried out were summarized. The major conclusions from each individual work are summarized in section 5.1, the scientific contributions are discussed in section 5.2, and the recommendation for future work are presented in section 5.3.

5.1 Summary

The conclusions of individual sections are summarized as follows:

5.1.1 Experimental study on direct adhesion warm roll-bonding metal-polymer-metal multilayer composites

In this work, AL1100-PU-AL1100 sandwich composites were successfully fabricated using a WRB process to achieve a direct bonding of layers without a glue agent. The effects of processing parameters included the surface roughness, preheat temperature, rolling speed, and thickness reduction on mechanical properties of the sandwich composites were investigated. The conclusions drawn from this study can be summarized as follows:

- Experimental results showed that mechanical interlocking was the primary direct adhesion mechanism in WRB process. Interface surfaces with high roughness values provided larger true surface area, and higher temperatures promoted deeper penetration of the polymer into the valleys of the metal surface, which led to higher adhesion strengths.
- The failure mode of warm roll bonded AL1100-PU laminate composite changed from adhesive to cohesive as the surface roughness increased.
- The bond strength increased with higher thickness reduction because of the increase in the mean contact pressure and more overlapping of exposed surface at the interface, but

excessive reduction at 75% led to inferior bonds due to the onset of mechanical instability.

- The presence of the soft PU layer in the AL1100-PU-AL1100 sandwich composite helps to increase the specific load compared with the AL1100 monolayer samples by 26%, 20%, and 36% at rolling thickness reductions of 50%, 60%, and 75%, respectively.
- At thickness reductions of 60% and 75%, the specific fracture energy of the sandwich composite improved by 10% and 20%, respectively.

5.1.2 Roll bonding of glass fiber reinforced metal-polymer-metal sandwich composites

The mechanical properties of warm roll bonded metal-polymer-metal sandwich composites with and without reinforced glass fiber have been measured and explained in this study. Conclusions from this study can be summarized as follows:

- The shear resistance of reinforced roll-bonded metal-polymer-metal sandwich composites at reductions of 60% and 75% enhanced by 39%, and 45%, respectively, when compared to the unreinforced composites.
- SPT results of the reinforced sandwich composites including ultimate load, specific load, and specific fracture energy improved by 18%, 19%, and 30%, respectively, when compared to the unreinforced composites at thickness reduction of 75%.
- Scanning electron microscope observations have confirmed the existence of the toughening mechanisms such as, fiber bridging, fiber pull-out, and fiber fracturing that contribute to enhance against shear failure of the roll-bonded metal-polymer sandwich composites.

5.2 Contributions

The major contributions of the dissertation may be summarized as the following:

- The AL1100-PU-AL1100 sandwich composite was successfully fabricated using direct adhesion warm roll-bonding technique for the first time. In addition, the effects of WRB process parameters including, surface roughness, rolling speed, preheat temperature, and thickness reduction on adhesion strength and mechanical properties were revealed.
- The small punch test (SPT) was employed to compare roll-bonded sandwich composites with mono-materials at the same thickness, and the results revealed significant improvements on the SPT results for the sandwich composites.
- In the roll-bonded AL1100-PU-AL1100 sandwich composite, the mechanical interlocking was identified as the governing mechanism for the adhesion at the metal-polymer interface.
- The s-glass fibers were successfully introduced at the interface of the laminated metal-polymer composite using the direct adhesion roll-bonding technique. The improvements on the mechanical and bonding properties of the reinforced roll-bonded sandwich composites were achieved.

5.3 Recommendations for the future work

The following topics are recommended for the future work.

1. Although the roll-bonded metal-polymer-metal sandwich composites have many advantages, the forming of these materials is complicated due to the large difference in the mechanical and thermal properties of the of the polymer core and the metal skins. The behavior of the sandwich sheets are quite different from those of homogeneous

metallic sheets. Understanding the formability of these composites is needed to produce final parts.

2. Many metal-polymer sandwich composites have been used in the automobile industries as passive dampers to reduce vibration and noise. Thus, understanding and investigating the vibration damping, impact response, and acoustic damping properties of the roll-bonded metal-polymer sandwich composites is crucial to facilitate their use in automobile and aeronautical industries.
3. Many applications like aircraft structures, car body parts and truck structures involve cyclic loading, which can degrade the mechanical properties of the sandwich composites and generate fatigue failure. Hence, an understanding of fatigue behavior is important prior to its use in these applications since no glue agent is used between the layers.

BIBLIOGRAPHY

- Abbasi, M., Toroghinejad, M.R., 2010. Effects of processing parameters on the bond strength of Cu/Cu roll-bonded strips. *Journal of Materials Processing Technology* 210, 560-563.
- Abdulmajeed, A.A., Närhi, T.O., Vallittu, P.K., Lassila, L.V., 2011. The effect of high fiber fraction on some mechanical properties of unidirectional glass fiber-reinforced composite. *dental materials* 27, 313-321.
- Baldan, A., 2012. Adhesion phenomena in bonded joints. *International Journal of Adhesion and Adhesives* 38, 95-116.
- Bryce, D.M., 1996. *Plastic injection molding: manufacturing process fundamentals*. Society of Manufacturing Engineers.
- Bulloch, J., 2004. A study concerning material fracture toughness and some small punch test data for low alloy steels. *Engineering failure analysis* 11, 635-653.
- Burchitz, I., Boesenkool, R., van der Zwaag, S., Tassoul, M., 2005. Highlights of designing with Hylite—a new material concept. *Materials & design* 26, 271-279.
- Carradò, A., Faerber, J., Niemeyer, S., Ziegmann, G., Palkowski, H., 2011a. Metal/polymer/metal hybrid systems: Towards potential formability applications. *Composite Structures* 93, 715-721.
- Carradò, A., Sokolova, O., Donnio, B., Palkowski, H., 2011b. Influence of corona treatment on adhesion and mechanical properties in metal/polymer/metal systems. *Journal of Applied Polymer Science* 120, 3709-3715.
- Carradò, A., Sokolova, O., Ziegmann, G., Palkowski, H., 2010. Press joining rolling process for hybrid systems, *Key Engineering Materials*. Trans Tech Publ, pp. 271-281.
- Carrado., A., Sokolova., O., Ziegmann., G., Plalkowski., H., 2010. Press Joining Rolling Process for Hybrid Systems. *Key Engineering Materials* 425, 271-281.
- Cheon, J.S., Kim, I.S., 1996. Initial deformation during small punch testing. *Journal of testing and evaluation* 24, 255-262.
- Davis, M.J., PSM, B., Eng, M., Director, R., 2010. **ASSESSING ADHESIVE BOND FAILURES: MIXED-MODE BOND FAILURES EXPLAINED.**
- DIN53281, 1979. Testing of adhesives for metal and adhesively bonded metal joints. T-peel test 09, 2.
- Dymáček, P., 2001. Fiber-metal laminates steel-C/epoxy. *Fiber-Metal Laminates Steel-C/Epoxy*.
- Edidin, A., Kurtz, S., 2001. Development and validation of the small punch test for UHMWPE used in total joint replacements, *Key Engineering Materials*. Trans Tech Publ, pp. 1-40.
- Gresham, J., Cantwell, W., Cardew-Hall, M.J., Compston, P., Kalyanasundaram, S., 2006. Drawing behaviour of metal–composite sandwich structures. *Composite Structures* 75, 305-312.

- Grujicic, M., 2014. Injection over molding of polymer-metal hybrid structures. *Am. J. Sci. Technol* 1, 167-181.
- Harhash, M., Carradò, A., Palkowski, H., 2017. Mechanical properties and forming behaviour of laminated steel/polymer sandwich systems with local inlays – Part 2: Stretching and deep drawing. *Composite Structures* 160, 1084-1094.
- Harris, B., 1978. Cracking in composites of glass fibres and resin, *Proceedings of the Royal Society of London A: Mathematical, Physical and Engineering Sciences*. The Royal Society, pp. 229-250.
- Harris, B., 2013. Micromechanisms of crack extension in composites. *Metal Science*.
- Herrmann, A.S., Zahlen, P.C., Zuardy, I., 2005. Sandwich structures technology in commercial aviation, *Sandwich structures 7: Advancing with sandwich structures and materials*. Springer, pp. 13-26.
- Honkanen, M., 2011. Injection-Molded Hybrids—Characterization of Metal-Plastic Interfacial Features. Tampereen teknillinen yliopisto. Julkaisu-Tampere University of Technology. Publication; 993.
- Institute of Metallurgy (IMET), TU Clausthal.
- Isselin, J., Shoji, T., 2009. Yield strength evaluation by small-punch test. *Journal of Testing and Evaluation* 37, 1-7.
- Jamaati, R., Toroghinejad, M., 2011. Cold roll bonding bond strengths: review. *Materials science and technology* 27, 1101-1108.
- Joachim Gähde, J.F.F., Rolf Gehrke, Ingrid Loeschcke & Jörg Sachse, 1992. Adhesion of polyurethane to surface-modified steel. *Journal of Adhesion Science and Technology* 6, 569-586.
- Johannaber, F., Johannaber, F., Johannaber, F., 1983. *Injection molding machines*. Hanser Munich.
- Kawai, M., Hachinohe, A., 2002. Two-stress level fatigue of unidirectional fiber–metal hybrid composite: GLARE 2. *International Journal of Fatigue* 24, 567-580.
- Kim, J.-K., Mai, Y.-w., 1991. High strength, high fracture toughness fibre composites with interface control—a review. *Composites Science and Technology* 41, 333-378.
- Kim, K.J., Kim, D., Choi, S.H., Chung, K., Shin, K.S., Barlat, F., Oh, K.H., Youn, J.R., 2003. Formability of AA5182/polypropylene/AA5182 sandwich sheets. *Journal of Materials Processing Technology* 139, 1-7.
- Kim, W.-S., Yun, I.-H., Lee, J.-J., Jung, H.-T., 2010. Evaluation of mechanical interlock effect on adhesion strength of polymer–metal interfaces using micro-patterned surface topography. *International Journal of Adhesion and Adhesives* 30, 408-417.
- Kopp, R., Nutzmann, M., van Santen, J., 2005. Formability of Lightweight, Vibration Damping and Medium Perfused Sandwich Sheets, *Sandwich Structures 7: Advancing with Sandwich Structures and Materials*. Springer, pp. 723-732.

- Lesuer, D., Syn, C., Sherby, O., Wadsworth, J., Lewandowski, J., Hunt, W., 1996. Mechanical behaviour of laminated metal composites. *International Materials Reviews* 41, 169-197.
- Link, T.M., 2001. Formability and performance of steel-plastic-steel laminated sheet materials. SAE Technical Paper.
- Lukaschkin, N., Borissow, A., Erlikh, A., 1997. The system analysis of metal forming technique in welding processes. *Journal of materials processing technology* 66, 264-269.
- Mak, J.C.K., 2011. Small punch testing of advanced metal matrix composites. University of Technology, Sydney.
- Mallick, P.K., 2007. Fiber-reinforced composites: materials, manufacturing, and design. CRC press.
- Moriwaki, T., 1996. Mechanical property enhancement of glass fibre-reinforced polyamide composite made by direct injection moulding process. *Composites Part A: Applied Science and Manufacturing* 27, 379-384.
- Mousa, S., Kim, G.-Y., 2015a. Direct Adhesion of Warm Roll-Bonded Al1100/Polyurethane/Al1100 Sandwich Composite, ASME 2015 International Manufacturing Science and Engineering Conference. American Society of Mechanical Engineers, pp. V001T002A101-V001T002A101.
- Mousa, S., Kim, G.-Y., 2015b. Experimental study on warm roll bonding of metal/polymer/metal multilayer composites. *Journal of Materials Processing Technology* 222, 84-90.
- Mousa, S., Kim, G.-Y., 2017. A direct adhesion of metal-polymer-metal sandwich composites by warm roll bonding. *Journal of Materials Processing Technology* 239, 133-139.
- Mower, T.M., Li, V.C., 1987. Fracture characterization of random short fiber reinforced thermoset resin composites. *Engineering fracture mechanics* 26, 593-603.
- Mukhopadhyay, M., 2005. Mechanics of composite materials and structures. Universities Press.
- Nadkarni, V., Ayodhya, S., 1993. The influence of knit-lines on the tensile properties of fiberglass reinforced thermoplastics. *Polymer Engineering & Science* 33, 358-367.
- Oertel, G., 1994. Polyurethane Handbook, Germany.
- Ohashi, Y., Wolfenstine, J., Koch, R., Sherby, O.D., 1992. Fracture behavior of a laminated steel-brass composite in bend tests. *Materials Science and Engineering: A* 151, 37-44.
- Packham, D.E., 1992. The Mechanical Theory of Adhesion—Changing Perceptions 1925-1991. *The journal of adhesion* 39, 137-144.
- Palkowski, H., Lange, G., 2005. Austenitic sandwich materials in the focus of research. Association of Metallurgical Engineers of Serbia, pp. 215-224.
- Pan, D., Gao, K., Yu, J., 1989. Cold roll bonding of bimetallic sheets and strips. *Materials science and technology* 5, 934-939.
- Peng, X.K., Heness, G., Yeung, W.Y., 1999. Effect of rolling temperature on interface and bond strength development of roll bonded copper/aluminium metal laminates. *Journal of Materials Science* 34, 277-281.

- Prolongo, S.G., Rosario, G., Ureña, A., 2006. Study of the effect of substrate roughness on adhesive joints by SEM image analysis. *Journal of Adhesion Science & Technology* 20, 457-470.
- Ramani, K., Moriarty, B., 1998. Thermoplastic bonding to metals via injection molding for macro-composite manufacture. *Polymer Engineering & Science* 38, 870-877.
- Reyes, G., Kang, H., 2007. Mechanical behavior of lightweight thermoplastic fiber–metal laminates. *Journal of materials processing technology* 186, 284-290.
- Rolfe, S.T., Barsom, J.M., 1977. *Fracture and fatigue control in structures: Applications of fracture mechanics*. ASTM International.
- Rowley, W.W., 2001. Method for manufacturing crosslinked overmolded plumbing tubes. Google Patents.
- Ruokolainen, R., Sigler, D., 2008a. The Effect of Adhesion and Tensile Properties on the Formability of Laminated Steels. *J. of Materi Eng and Perform* 17, 330-339.
- Ruokolainen, R.B., Sigler, D.R., 2008b. The effect of adhesion and tensile properties on the formability of laminated steels. *J. of Materi Eng and Perform* 17, 330-339.
- Sokolova, O., Carradó, A., Palkowski, H., 2010. Production of customized high-strength hybrid sandwich structures, *Advanced materials research*. Trans Tech Publ, pp. 81-128.
- Sokolova, O.A., Carradó, A., Palkowski, H., 2011. Metal–polymer–metal sandwiches with local metal reinforcements: A study on formability by deep drawing and bending. *Composite Structures* 94, 1-7.
- Soltan Ali Nezhad, M., Haerian Ardakani, A., 2009. A study of joint quality of aluminum and low carbon steel strips by warm rolling. *Materials & Design* 30, 1103-1109.
- Standard, A., 2007a. *Metallic materials—Tensile testing at ambient temperature*. 1391: 2007.
- Standard, A., 2007b. *Metallic materials—tensile testing at ambient temperature*. AS 1391-2007, Australia.
- Suresh, S., 1983. Crack deflection: implications for the growth of long and short fatigue cracks. *Metallurgical Transactions A* 14, 2375-2385.
- Tang, W., Santare, M.H., Advani, S.G., 2003. Melt processing and mechanical property characterization of multi-walled carbon nanotube/high density polyethylene (MWNT/HDPE) composite films. *Carbon* 41, 2779-2785.
- Thomsen, O.T., Bozhevolnaya, E., Lyckegaard, A., 2006. *Sandwich Structures 7: Advancing with Sandwich Structures and Materials: Proceedings of the 7th International Conference on Sandwich Structures*, Aalborg University, Aalborg, Denmark, 29-31 August 2005. Springer Science & Business Media.
- Wang, Z.-X., Shi, H.-J., Lu, J., Shi, P., Ma, X.-F., 2008. Small punch testing for assessing the fracture properties of the reactor vessel steel with different thicknesses. *Nuclear Engineering and Design* 238, 3186-3193.

- Watabe, Y., Ishii, M., Iseda, Y., 1977. Polyurethane composition having improved tear strength and process for preparation thereof. Google Patents.
- Winandy, J.E., Kamke, F.A., 2004. Fundamentals of composite processing: proceedings of a workshop. US Dept. of Agriculture, Forest Service, Forest Products Laboratory.
- Yang, B., Nunez, S.W., Welch, T.E., Schwaegler, J.R., 2001. Laminate dash ford taurus noise and vibration performance. SAE Technical Paper.
- Yue, C., Cheung, W., 1992. Interfacial properties of fibre-reinforced composites. *Journal of materials science* 27, 3843-3855.
- Ziegmann, G., 1998. Advance Materials and Design Procedure for Large Size SES Structures. European Researchproject BRE2-0582, Project BE-7651, annual report.
- Zoellner, O., Evans, J., 2002. Plastic-Metal Hybrid-A new development in the injection molding technology (37), ANTEC-CONFERENCE PROCEEDINGS-. UNKNOWN, pp. 2966-2969.